Acurex Corporation/Aerotherm Division

March 1976

Aerotherm Project 7084

UNIFIED COMPUTER CODES
PROPERTIES DATA FOR LOW COST NOZZLE MATERIALS

E. Chu
H. Tong
R. Bedard

AEROTHERM REPORT TR-76-9

Prepared for

National Aeronautics and Space Administration
Marshall Space Flight Center
Huntsville, Alabama 35812

Contract NAS8-30264

ACUREX Aerotherm

TABLE OF CONTENTS

LIST OF ILLUSTRATIONS

LIST OF ILLUSTRATIONS (Concluded)

LIST OF TABLES

SECTION 1

INTRODUCTION AND SUMMARY

Rocket nozzles for the Space Shuttle SRM are being designed using materials which have been proven successful by many years of testing. However, the Shuttle philosophy of providing an economical means of placing material and personnel into earth orbit requires a continued effort to reduce mission costs. One area in which significant cost reductions can be realized is in the area of the nozzle ablative liners. The primary high heat load material for current nozzles is a rayon precursor carbon phenolic (e.g., Fiberite MX 4926). The material for lower heating conditions in the exit cone and nozzle backside is a silica phenolic (e.g., Fiberite MX 2600). Over the past several years, a number of low cost materials have been proposed as substitutes for the above materials; however, the level to which these materials have been characterized was insufficient to allow a thermal analysis of a full scale nozzle design. A need therefore existed to obtain the thermophysical and thermochemical properties of promising low cost materials.

Low cost carbon phenolic materials development has centered on the replacement of rayon precursor carbon with pitch precursor carbon. Using continuous filament pitch carbon fabrics, the projected costs for carbon phenolic in the early 1980's may be about 23$/pound. Using pitch carbon mats, the cost may decrease to as low as 12$/pound. Further reductions may be possible as pitch carbon makes a deeper penetration into consumer goods. These projected costs may be compared to about 30$/pound for current carbon phenolic prepreg.

Low cost materials development to replace current silica phenolics has centered on the use of double thickness cloths and elastomeric resins to increase the component fabrication speed. Material costs are not projected to be altered significantly in the next decade. Alternative reinforcements, such as canvas, have also been considered.

The objective of this investigation was to develop the analytic capability to predict the thermal ablation response of promising low cost materials. To achieve this objective, it was necessary to

1. Select potentially viable low cost materials. This was accomplished by a questionnaire and telephone survey of material prepreggers and nozzle fabricators.

2. Experimentally determine the relative thermal performance of these materials. This was accomplished by screening potential low cost materials in the Aerotherm arc plasma generator.

3. Determine if materials of the same generic class but from different suppliers performed differently. This was determined from the screening test data.

4. Select representative materials from each generic class and determine their thermophysical and thermochemical properties. This was accomplished by appropriate characterization experiments.

5. Define these characteristics in a form which is compatible with current thermal performance prediction techniques.

In the arc plasma generator ablation tests performed in Steps 2 and 4, Fiberite MX 4926 (carbon phenolic) and MX 2600 (silica phenolic) were used as reference baseline materials. For the low cost materials primary emphasis was on pitch carbon reinforced phenolics; however silica and canvas reinforced phenolics were also tested.

The generic classes of materials selected for low cost evaluation were

1. Pitch carbon mat reinforced phenolic

2. Pitch carbon fabric reinforced phenolic

3. Pitch carbon molding compound

4. Hybrid pitch carbon mat/rayon carbon cloth reinforced phenolic

5. Silica reinforced phenolics

6. Canvas cloth reinforced phenolic.

Phenolic or elastomer modified phenolic was the resin for each generic class. Materials were obtained from a number of prepreg suppliers. These materials were quantitatively compared in terms of thermal performance by a simulation of propellant environments in an arc plasma generator. It was found that material response was not very dependent upon the supplier of the material; however, a dependence on cure cycle was observed.

In order to provide data for analytic purposes, the thermophysical properties of these low cost materials were evaluated. These data were assembled in a form which is compatible with current prediction procedures. As a result of this program an analytic capability has been established to predict the thermal performance of new low cost rocket nozzle liner materials.

Aerotherm is pleased to acknowledge the cooperation and contributions of the Fiberite, Ferro, Hexcel and U.S. Polymeric Corporations. These organizations responded to a lengthy questionnaire and provided all of the required test materials.

SECTION 2

MATERIAL SURVEY STUDY

Since there is only limited knowledge of the performance of low cost materials in rocket nozzles, a material survey study was necessary to capitalize on the background of material suppliers. Such a survey study will not only enable one to have a better understanding of the thermal behavior of low cost materials, it will also provide a better perspective in designing a test matrix for the low cost materials performance study.

The survey study started with data collection. Material manufacturers and nozzle fabricators were contacted to participate in this program and to propose promising low cost materials. The companies which responded were as follows:

- Fiberite Corporation
- Hexcel Corporation
- U. S. Polymeric Corporation
- Ferro Corporation

Questionnaires covering the areas such as material properties, fabrication techniques, cure procedure, and material characteristics were sent to the above companies for their response. This information was subsequently compiled and integrated qualitatively into a screening test matrix.

The second part of the survey study was to perform a qualitative analysis on the proposed low cost materials based upon the information received. By utilizing mechanical and thermal properties from qualified materials (MX 4926 – Shuttle SRM baseline throat material, MX 2600 – Shuttle SRM baseline exit cone material) as a guideline to analyze the proposed materials, less favorable materials were eliminated before the screening test.

The results of this study are shown in Tables 2-1 and 2-2. As can be seen, the properties of the selected low cost materials are of the same order of magnitude as the qualified materials.

Information on the cost of some of the selected screening materials was also collected from the above companies. An estimated trend of cost for each generic class of materials for calendar years between 1975 to 1987 are presented in Figure 2-1.

TABLE 2-1. CANDIDATE LOW COST MATERIALS FOR SHUTTLE SRM THROAT MATERIAL SCREENING TEST

Generic Title	Source	Material Designation	Density (GR/CC)	Resin Content (%)	Tensile Strength (KSI)	Tensile/ Flexure Modulus (MSI)	With Ply Conductivity $\frac{\text{Btu - in}}{\text{Hr-Ft}^{-2}\text{F}}$	Volatile[1] Content (%)
Rayon Carbon Cloth Phenolic	Fiberite	MX 4926	1.40	34	18.0	2.7	3.5	0.56
Pitch Mat Carbon Phenolic	Fiberite USP Ferro	MX 4929 FM 4782BG ACX-C86PM	1.40 1.48 1.40	50 45 43	10.0 12.0	2.0 2.4	3.6 4.5 5.0	1.30 2.05 1.38
Hybrid Pitch Mat/Rayon Cloth Phenolic	Fiberite USP Hexcel	MX 4928 FM 5790 4CS P08/4C1008	1.40 1.50	52 44 45	10.0 13.5	2.0 2.5	6.7	1.70 2.81 1.47
Kynol Carbon Cloth Phenolic	USP Ferro	XFM 5795 ACX-CPH	1.49	36 41	15.0	2.5	4.5	5.41 1.46
Kureha Pitch Carbon Cloth Phenolic	Ferro	ACX-C86K		42				4.04
Pitch Mat Molding Compound	Fiberite USP Hexcel	MXC313P FM 5782 MC 4CS P08MC	1.50 1.60 1.50	37 38 45	7.0 6.0 9.5	2.0 2.4 2.2	2.5 5.5	1.08 1.76 1.69
Kureha Pitch Fabric Molding Compound	Ferro	ACX-C86KMC	1.40	46			5.8	2.33
Pitch Carbon Cloth Phenolic	Fiberite USP Hexcel	MXG 1033F FM 5795 4C 1246	1.64	32	23.5	5.0	2.5	3.80 5.41
US Pitch Fabric Molding Compound	Fiberite	MXG 1033FMC						

[1]Cured composite

TABLE 2-2. CANDIDATE LOW COST MATERIALS FOR SHUTTLE SRM EXIT CONE MATERIALS SCREENING TEST

Generic Title	Source	Material Designation	Density (GR/CC)	Resin Content	Against Ply Conductivity $\frac{\text{Btu - in}}{\text{Hr - Ft}^2{}^\circ\text{F}}$
Standard Silica Cloth Phenolic	Fiberite	MX 2600	1.74	33	4.1
Snapwrap Silica Cloth Phenolic	Fiberite	MXSE-55	1.30	30	2.2
Double Thick Silica Cloth Phenolic	Ferro	CA-2221/96	1.75	31	2.7
Canvas Cloth Phenolic	Fiberite Hexcel	MXKF-418 4K9502	1.30 1.20	38 42	2.2 -

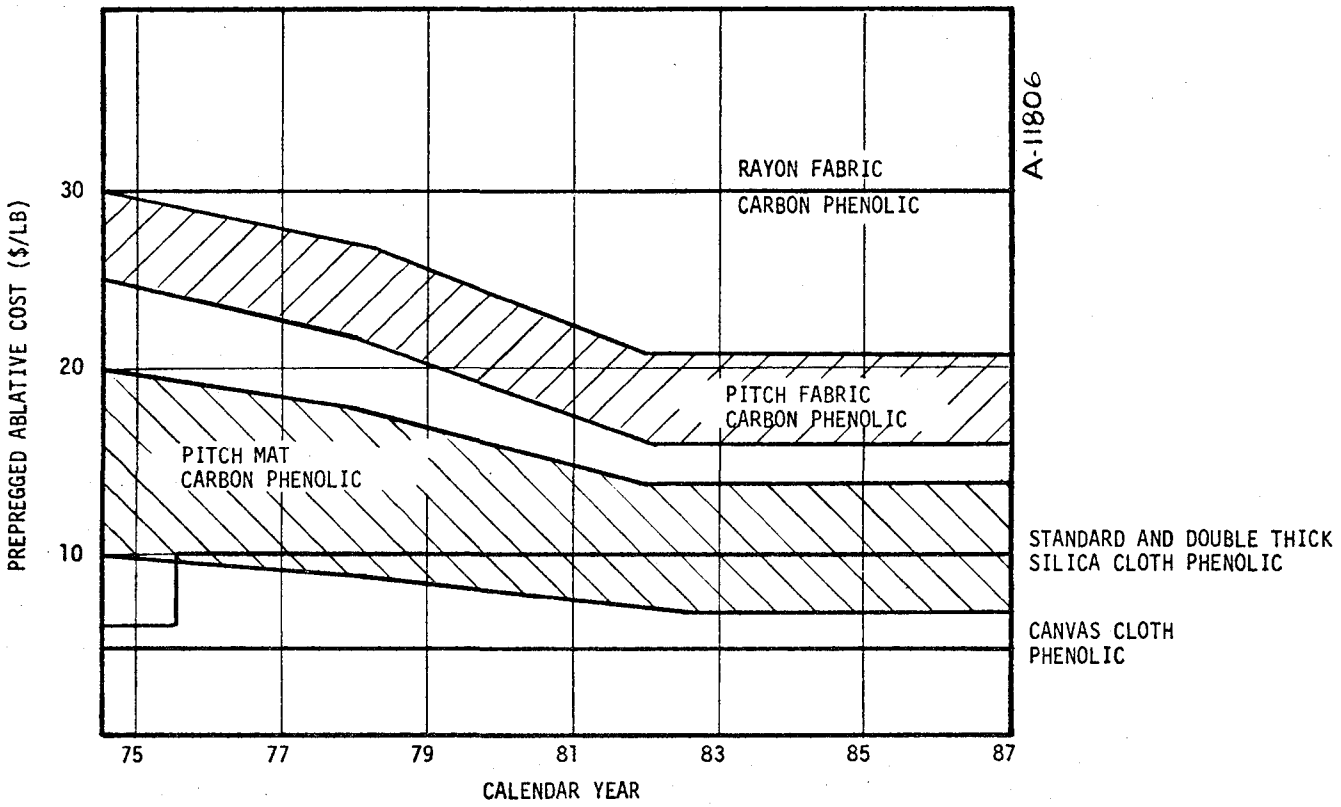

Figure 2-1. Prepregged ablative material raw costs.

SECTION 3

SUB-SCALE SCREENING TESTS

The thermal performance of a number of low cost materials was evaluated by a screening test program using an arc plasma generator (APG) as a convective heat source. The low cost materials in this program (see Tables 3-1 and 3-2) included pitch carbon phenolic candidate throat materials, and silica and canvas phenolic candidate exit cone materials. A major part of the screening program was devoted to the pitch carbon phenolics since these materials show promise for very significant reductions in material costs.

The screening test conditions were designed to simulate the actual motor firing conditions as closely as possible. Since the major emphasis was the thermal performance of a meterial in a rocket nozzle, simulation of the following parameters was considered important:

- Heat flux to the material (q)
- Reactive chemical species (H, O) composition

These two parameters were chosen because the former represents the simulation of in-depth temperature profile and the latter represents the simulation of surface chemical erosion. An exact simulation would, of course, not be possible so some compromises were necessary for testing in an arc plasma generator. Tables 3-1 and 3-2 show the comparisons between the screening test conditions and anticipated motor firing conditions.

Low cost materials were tested in the APG in a planar nozzle configuration (see Figure 3-1). As can be seen two samples can be tested simultaneously. Due to supplier difficulties, not all of the materials selected for screening tests were received in time. The screening tests were therefore performed in two series. Series I screening tests were performed with the composite plies in the 0 degree orientation for exit and molding compound materials and 90 degree orientation for throat materials. Continuous filament pitch carbon phenolic material (Series II) was tested in the 90° orientation with a dummy model on the opposite wall. These dummy models were fabricated from the same materials but plies were oriented at 20° rather than 90°. A tentative selection of materials for full characterization was made based on the first screening test series.

TABLE 3-1. COMPARISON OF ROCKET MOTOR AND APG ENVIRONMENTS

Rocket Motor Convective Environment

$\frac{A}{A^*}$	λ (ft)	p_e (atm)	u_e (ft/sec)	h_e (Btu/lbm)	$\rho_e u_e C_H$ (lbm/ft²-sec)	q (Btu/ft²-sec)
1.0	3.1	26	3430	595	0.78	1170
3.0	7.8	3.2	7050	-190	.21	277
4.0	9.6	2.2	7440	-320	.15	265

ARC Plasma Generator Environment

$\frac{A}{A^*}$	p_e (atm)	h_e (Btu/lbm)	$\rho_e u_e C_H$ (lbm/ft²-sec)	q_{cw} (Btu/ft²-sec)
1.0	2.93	8713	0.074	982
3.0	1.82	2456	.042	281
4.0	1.76	2558	.037	250

TABLE 3-2. COMPARISON OF APG TEST GAS AND TYPICAL NOZZLE EXHAUST GAS EQUILIRBIUM COMPOSITION

Test Gas Equilibrium Composition
$2\ H_2O + CO + 8.3\ H_2$
Typical Nozzle Exhaust Gas H, C, O Equilibrium Composition
$2\ H_2O + CO$

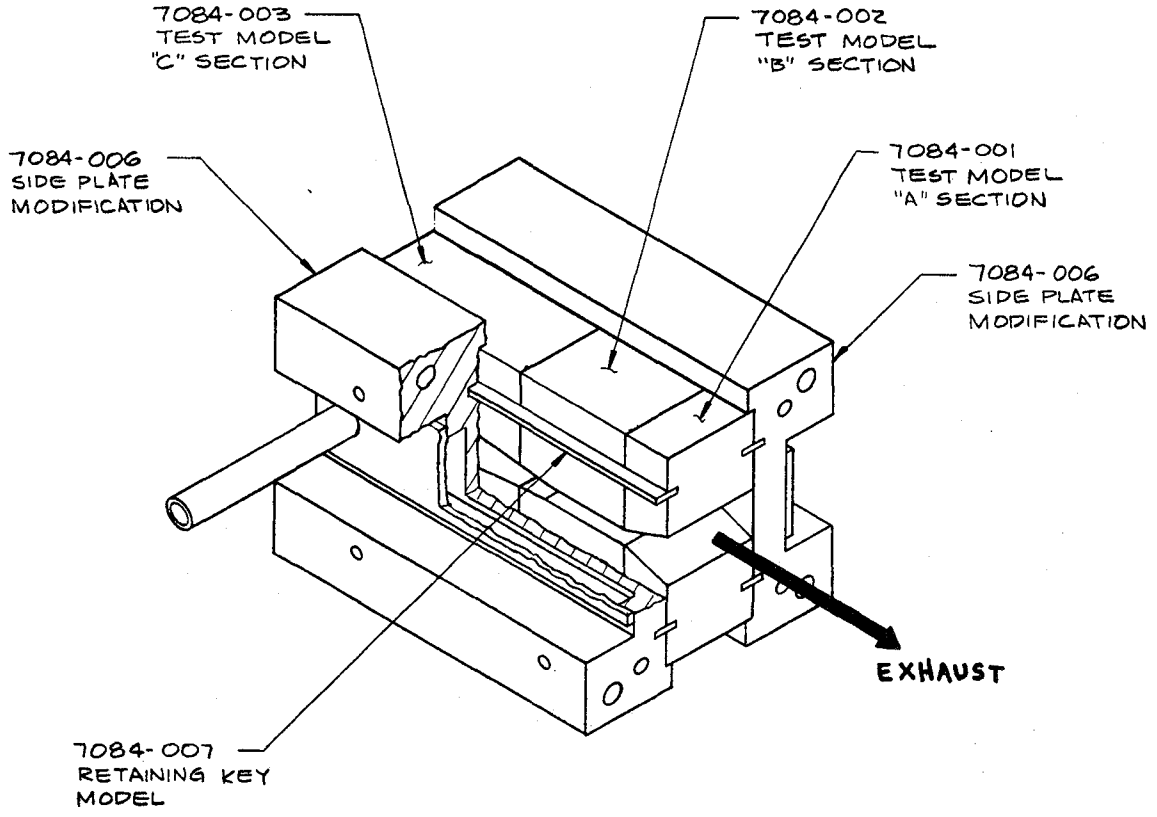

Figure 3-1. Test configuration.

In the Series I tests, the throat entrance insert ("C" section) was fabricated from pyrolytic graphite. Very little ablation was observed on this section so that subsequent Series II testing was done using P03 graphite throat entrance inserts. However, as a precaution, the inlet end of the throat test section was increased to minimize any possible effects due to material discontinuities. The test configurations for both Series I and II are shown in Figure 3-2 and the test matrix is shown in Table 3-3. As can be seen, materials from the same generic class were arranged to be tested simultaneously on the premise that their performance should be similar.

The screening test results are shown in Tables 3-4 and 3-5 respectively for pitch and silica-reinforced material. As can be seen, the ablation performance of the selected low cost materials for tha Shuttle SRM throat were all comparable to the baseline material, rayon carbon cloth phenolic. In fact, some materials appeared to be even superior to rayon precursor carbon cloth phenolic. Some similarity in ablation performance is expected because the thermal and physical properties of the tested materials were of the same order of magnitude (see Table 2-1), however superior performance was an unexpected benefits. Typical post-test surface conditions for some APG screening test samples are shown in Figure 3-3 to 3-5.

The screening test results for Shuttle SRM exit cone materials indicate that (see Table 3-5) double thick silica cloth phenolic had the best ablation performance among the silica cloth phenolic materials. The reason for this superior performance is not clear because no correlation was found based on the material properties. Canvas cloth phenolic has poorer performance compared to silica cloth phenolic. The reason here is obvious; canvas cloth phenolic has higher hydrogen and oxygen contents which result in a higher degree of thermal decomposition.

Also shown in Tables 3-4 and 3-5 are the residual volatiles content for the cured composites tested in Series I. These measurements were made by Hexcel Corporation.

From the screening test results, five generic materials were selected for full thermophysical property characterization. Of these five, four were selected from the throat material category and one from the exit cone material category. Since the main objective of this program was to study low cost materials, the selection was based on ablation performance as well as cost performance. Cost performance here is defined as total ablation times material cost per pound. During the first round of selection, one representative material from each generic title was selected based on ablation performance. On the second round of selection, a comparison of cost performance among the representative materials was made (see Tables 3-6 and 3-7), and the five materials were selected accordingly.

Screening Test Series 1

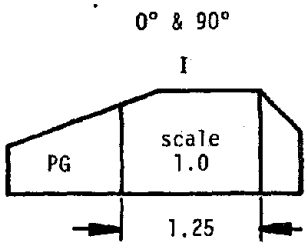

Screening Tests Series 2

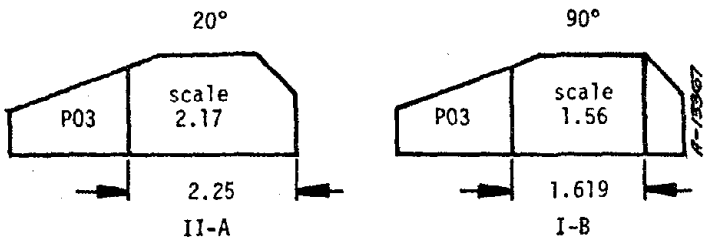

Figure 3-2. Screening test sample dimensions.

TABLE 3-3. SCREENING TEST MATRIX

Series	Test No.	Model Description		Orientation (Deg.)
I	2524	FM5782MC	MXC313P	0
	2525	4CSP08MC	ACS-C86PMC	
	2530	4CSP08MC	ACS-C86PMC	
	2534	MX2600	CA-2221	
	2535	MX2600	MXSE-55	
	2536	MX2600	4K9502	
	2537	MX2600	MXKF-418	
	2541	MX4926	ACX-C86PM	90
	2542	ACX-C86K	ACX-C861C	
	2543	XFM5795	ACX-CPH	
	2544	MX-4929	FM5782BG	
	2545	4CSP08/4C1008	MX4926	
	2546	MX4928	FM5790	
II	1	DUMMY	4C1246 90°	
		DUMMY	FM5795 90°	
		DUMMY	MXG1033FMC 90°	

TABLE 3-4. SHUTTLE SRM THROAT MATERIAL SCREENING TEST RESULTS

Generic Title	Source	Material Designation	Volatile[2] Content (%)	Mass[3] Loss (Grams)	Surface Appearance
Rayon Cloth Cloth Phenolic	Fiberite	MX4926	0.56	5.2	Smooth
Pitch Mat Carbon Phenolic	Fiberite U.S. Polymeric Ferro	MX4929 FM5782BG ACX-C86PM	1.30 2.05 1.38	4.9 4.4 5.0	Smooth Smooth Smooth
Hybrid Pitch Mat/Rayon Cloth Phenolic	Fiberite U.S. Polymeric Hexcel	MX4928 FM5790 4CSP08/4C1008	1.70 2.81 1.47	4.8 4.0 5.3	Rough Rough Rough
Kynol Carbon Cloth Phenolic	Fiberite Ferro	XFM5795 ACX-CPH	5.41 1.46	3.6 3.3	Smooth Smooth
Kureha Pitch Carbon Cloth Phenolic	Ferro	ACX-C86K	4.04	5.8	Rough
Pitch Mat[1] Molding Compound	Fiberite U.S. Polymeric Hexcel	MXC-313P FM5782MC 4CSP08MC	1.08 1.76 1.69	5.7 6.8 6.6	Spalled Spalled Spalled
Kureha Pitch[1] Fabric Molding Compound	Ferro	ACX-C86KMC	2.33	4.1	Rough
Pitch Carbon Cloth Phenolic	Fiberite U.S. Polymeric Hexcel	MXC1033F FM5795 4C1246	3.80 5.41	(4) 4.6 5.2	
UC Pitch Fabric Molding Compound	Fiberite	MSG1033FMC		6.4	Rough

[1]Fabric plies were oriented 90° to the heated surface except for these materials. For these materials, the heated surface was perpendicular to the molding direction.

[2]Cured composite

[3]Normalized to 30 seconds and Series I configuration

[4]APG malfunction

TABLE 3-5. SHUTTLE SRM EXIT CONE MATERIALS SCREENING TEST RESULTS[1]

Generic Title	Source	Material Designation	Volatile Content (%)	Mass Loss (GMS)	Surface Appearance
Standard Silica Cloth Phenolic	Fiberite	MX2600	4.19	2.6	SiO_2 and SiC Formation
Snapwrap Silica Cloth Phenolic	Fiberite	MXSE-55	1.83	3.6	SiO_2 and SiC Formation
Double Thick Silica Cloth Phenolic	Ferro	CA-2221/96	2.22	1.8	SiO_2 and SiC Formation
Canvas Cloth Phenolic	Fiberite Hexcel	MXKF-418 4K9502	4.12 4.26	5.1 6.2	Significant Charring

[1]All tests conducted in the 0° ply orientation with respect to centerline

[2]Normalized to 30 seconds

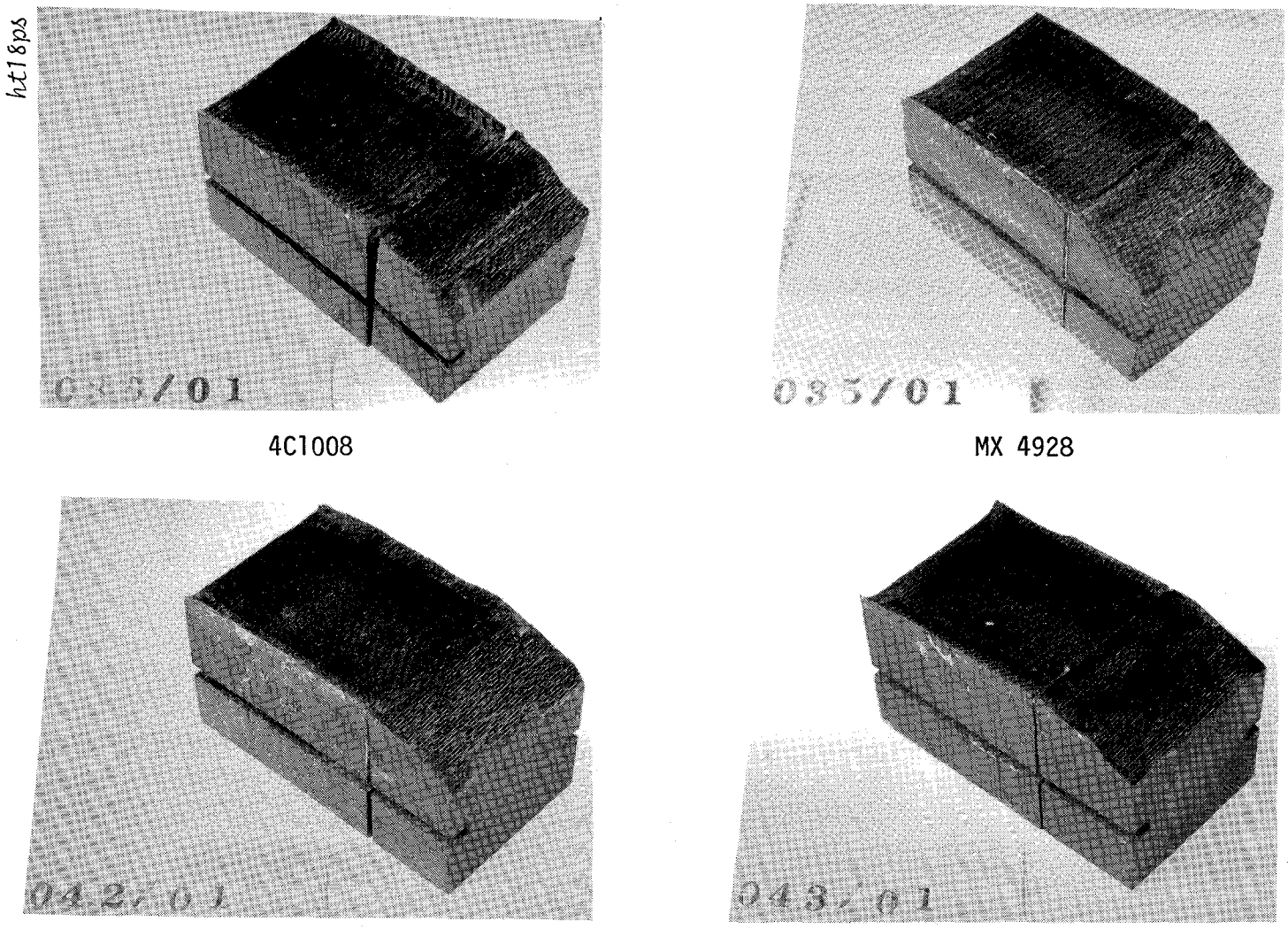

Figure 3-3.
Typical post-fired surface condition of hybrid carbon/phenolic materials.

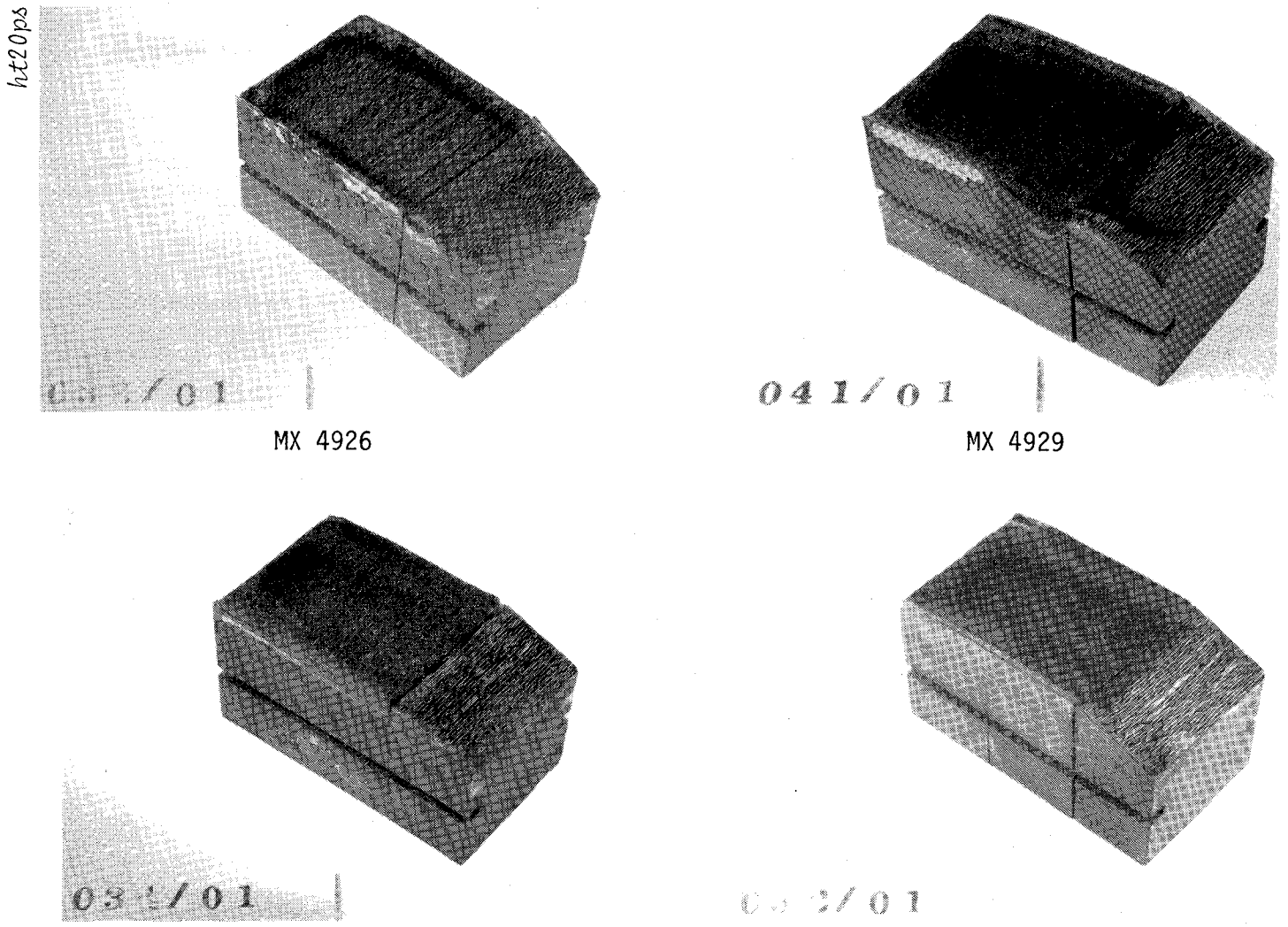

Figure 3-4.
Typical post-fired surface condition of pitch mat/phenolic materials.

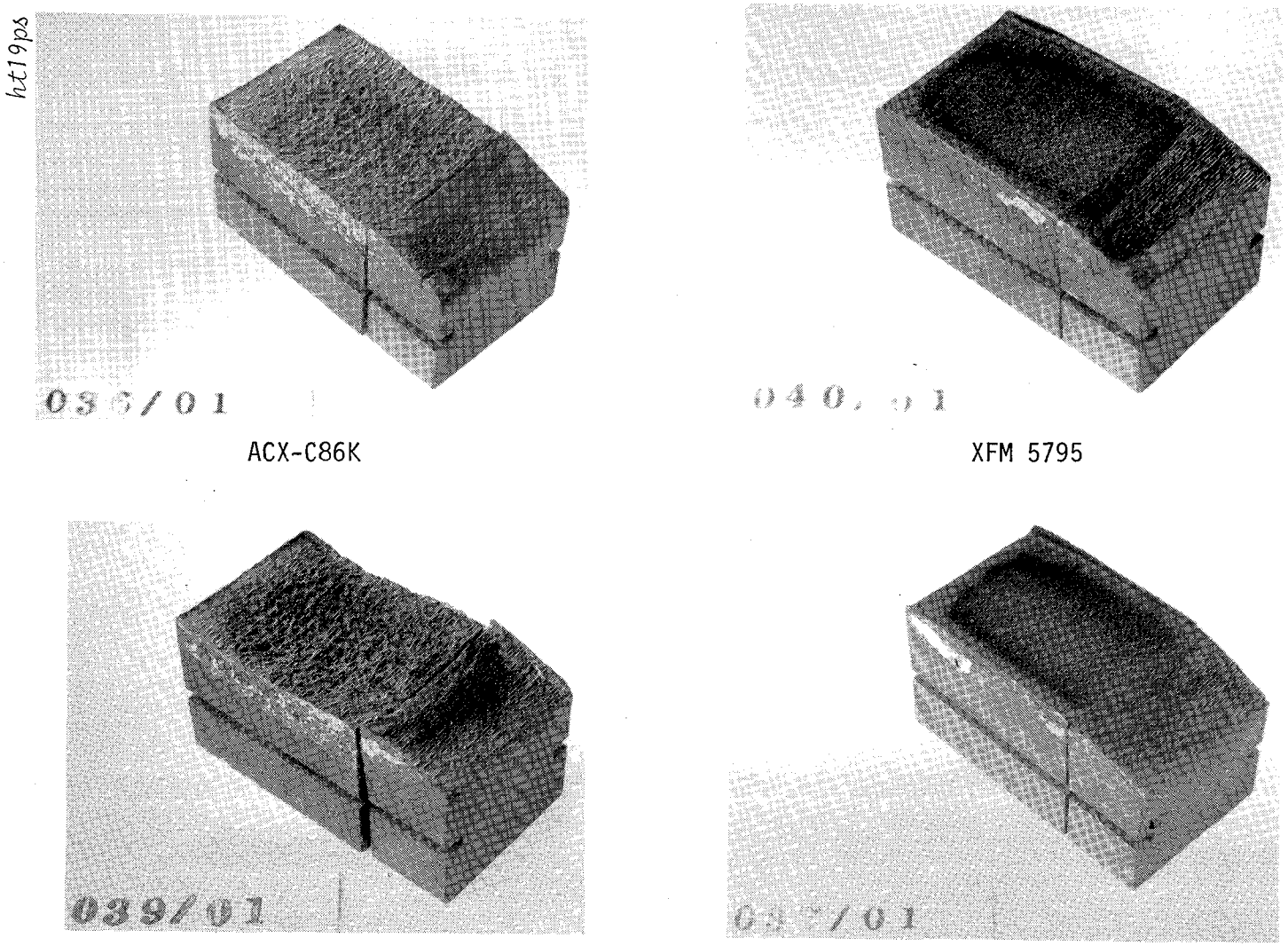

ACX-C86K

XFM 5795

ACX-686K

ACX-CPH

Figure 3-5. Typical post-fired surface condition of carbon fabric/phenolic materials.

TABLE 3-6. SHUTTLE SRM THROAT MATERIALS PERFORMANCE AND COST COMPARISONS

Generic Title	Nominal Density (GM/CC)	Nominal Mass Loss (GM)	Raw Material Cost (1975 $/lb)		Mass Loss x Raw Material Cost Performance (GMS x $/lb)	
			1975	1980	1975	1980
Rayon Carbon Cloth Phenolic	1.40	5.2	30.0	30.0	156	156
Pitch Mat Carbon Phenolic	1.45	4.8	15.0	12.0	72	58
Hybrid Pitch Mat/Rayon Cloth Phenolic	1.45	4.7	22.5	21.0	106	99
Kynol Carbon Cloth Phenolic	1.49	3.5	25.0	30.0	88	105
Kureha Pitch Carbon Cloth Phenolic		5.8				
Pitch Mat Molding Compound	1.53	6.3	15.5	12.5	98	79
Kureha Pitch Fabric Molding Compound	1.40	4.1				
UC Pitch Fabric Molding Compound		6.4	28.0	23.0	179	147

TABLE 3-7. SHUTTLE SRM EXIT CONE MATERIALS PERFORMANCE AND COST COMPARISONS

Generic Title	Nominal Density (GMS/CC)	Nominal Mass Loss (GMS)	Raw Material Cost (1975 $/lb)		Mass Loss x Raw Material Cost Performance (GMS x $lb)	
			1975	1980	1975	1980
Silica Phenolic	1.74	2.6	6	10	16	26
Snapwrap Silica Phenolic	1.30	3.6	6	10	22	36
Double Thick Silica Phenolic	1.75	1.8	6	10	11	18
Canvas Phenolic	1.25	5.6	5	5	28	28

The final selection of low cost materials for further study is shown in Table 3-8. With the exception of MXG1033F and 4K9502, these selected materials have shown good ablation performance and low cost potential. MXG1033F was selected arbitrarily since no screening test data was obtained for this material class. Silica phenolic is an obvious exit cone material; however low cost silica materials are very similar to those that have been previously characterized. Canvas phenolic was therefore selected as an exit cone material for full characterization. Canvas cloth phenolic has a reasonable low cost potential although quality control and material traceability leaves something to be desired.

TABLE 3-8. SELECTION OF SHUTTLE SRM LOW COST NOZZLE EVALUATION MATERIALS

Generic Title	Source	Material Designation
Pitch Fabric Carbon Phenolic	Fiberite	MXG 1033F
Pitch Mat Phenolic	Hexcel	4CS P08
Hybrid Pitch Mat/ Rayon Fabric Carbon Phenolic	U.S. Polymeric	FM 5790
Pitch Mat Phenolic Molding Compound	Fiberite	MXC 313P
Canvas Cloth Phenolic	Hexcel	4K 9502

SECTION 4

INTERMEDIATE TEST PROGRAM

In the low cost materials screening test, five generic materials (see Table 3-8) were selected for further evaluation. Both 20° and 90° composite ply orientation tests were performed on each of the five intermediate test materials. In addition, some materials were subjected to an extended cure* to determine whether or not this would affect the ablation performance.

The intermediate test matrix is shown in Table 4-1. The test configuration was the same as Series II of the screening test program.

TABLE 4-1. INTERMEDIATE TEST MATRIX

CARBON PHENOLIC, A/A* = 1.0			
90° orientation			
MXG1033F	A.R.*	MXG1033F	P.C.†
FM5790	A.R.	FM5790	P.C.
MXC313P	A.R.	MXC313P	P.C.
4CSP08	A.R.	4CSP08	P.C.
20° orientation			
MXG1033	A.R.	MXG1033F	P.C.
FM5790	A.R.	FM5790	P.C.
MXC313P	A.R.	MXC313P	P.C.
4CSP08	A.R.	4CSP08	P.C.
CANVAS PHENOLIC			
90° orientation			
4K9502	A.R.	4K9502	P.C.
20° orientation			
4K9502	A.R.	4K9502	P.C.

*As received material

†Post-cured material

*To be referred to as post-cured material.

The intermediate test results are shown in Table 4-2.

TABLE 4-2. SHUTTLE SRM EVALUATION MATERIALS INTERMEDIATE TEST RESULTS[1]

Generic Title	Source	Material Designation	20°[2] Mass Loss (GMS)	90°[2] Mass Loss (GMS)	A/A*[3]
Pitch Mat Carbon Phenolic	Hexcel	4CSP08	2.9	4.8	1.0
Hybrid Pitch Mat/Rayon Fabric Phenolic	USP	FM5790	2.5	4.5	1.0
Pitch Fabric Phenolic	Fiberite	MXG1033F	Test Facility Failure		1.0
Pitch Mat Molding Compound	Fiberite	MXC313P	2.6	6.0	1.0
Canvas Phenolic	Hexcel	4K9502	4.6	5.2	4.0

[1]All tests conducted in both the 20° and 90° ply orientation

[2]Normalized to 30 seconds and initial screening configuration, material as received

[3]Simulated Shuttle SRM nozzle expansion ratio

No delamination was observed in the 20° orientation for both cured (as received) and post-cured materials. It was also found that the post-cured materials (except for pitch mat molding compound) perform slightly better than the as-received materials (see Figures 4-1 and 4-2). The better performance is probably due to lower volatile and water contents in the post-cured materials since these two elements would induce exothermic reactions and chemical erosion at the surface. The results of the 90° orientation as-received materials did not provide any new information, but do provide assurance that materials to be fully characterized have a reproducible thermal performance.

The following conclusions can be extracted from this study.

- Intermediate test data are consistent with screening test data.
- The tests provided assurance that materials to be fully characterized are reproducible.
- Post-cured materials have better ablation performance than as-received materials.
- The results indicate that full characterization tests should be performed on post-cured materials.

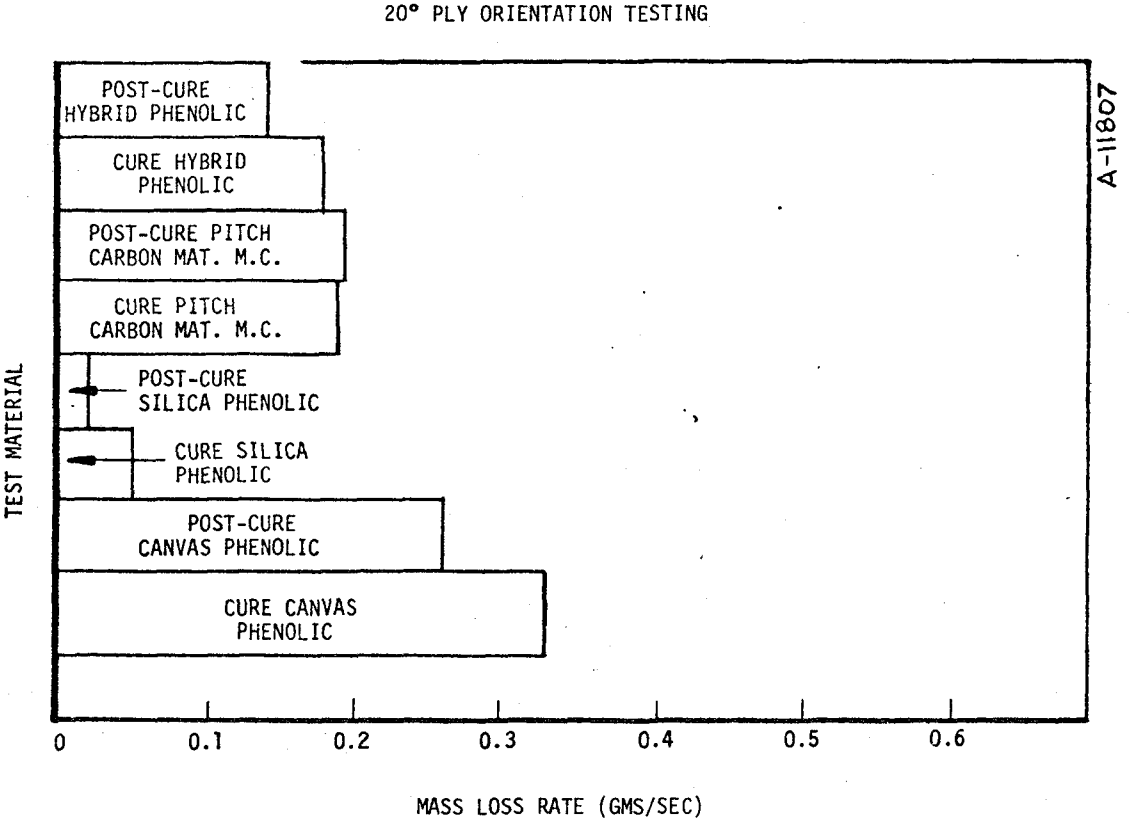

Figure 4-1. Cured versus post-cured intermediate test results.

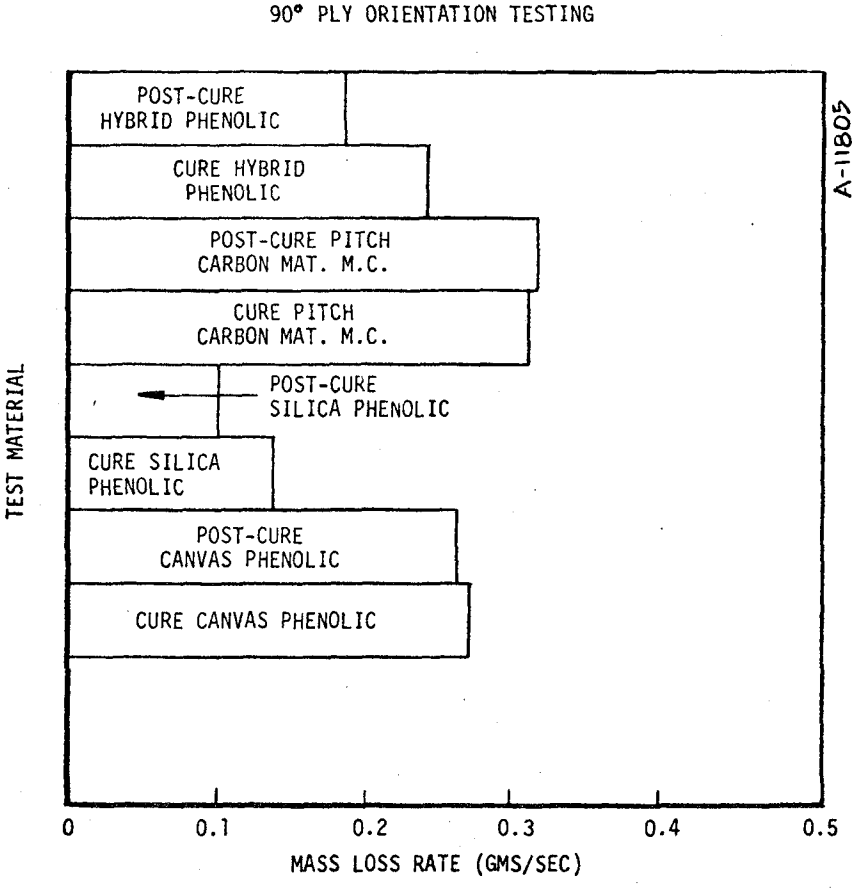

Figure 4-2. Cured versus post-cured intermediate test results.

SECTION 5

MATERIALS FULL CHARACTERIZATION PROGRAM

Since the properties for charring ablative materials are dependent upon fabric orientation and thermodynamic state (T and ρ), material properties were evaluated for virgin and charred composites in at least two fabric orientations. The properties determined were

- Decomposition kinetics
- Elemental composition
- Heat of formation
- Density
- Specific heat capacity
- Thermal conductivity

The materials for which these properties were determined are

- U.S. Polymeric FM5790
- Fiberite MXG1033F
- Hexcel 4K9502
- Fiberite MXC313P
- Hexcel 4CSP08

5.1 DECOMPOSITION KINETICS

Resinous materials degrade in a highly complex manner. These complex degradation mechanisms are generally not understood sufficiently to formulate exact analytical expressions. Therefore, empirical homogeneous kinetics are normally used to describe the degradation.

The thermal degradation reactions, if assumed to be irreversible, may be described by a psuedo-order classical rate expression.

$$\frac{\partial \rho_i}{\partial \theta} = -B_i \exp\left(-\frac{E_{ai}}{RT}\right) \rho_{oi} \left(\frac{\rho_i - \rho_{ri}}{\rho_{oi}}\right)^{\psi_i} \tag{5-1}$$

The kinetic parameters (activation energy E_{ai}, frequency factor B_i, and reaction order ψ_i) can be determined by reducing thermogravimetric analysis (TGA) data.

The multiple-linear-regression analysis is one of the procedures which can be used to reduce TGA data. This analysis has the capability to evaluate the three kinetic parameters simultaneously and also to curve fit the input data in a theoretically optimal manner.

The evaluation procedure is straightforward. Equation (5-1) is first linearized to yield the following form

$$\ell n \left(-\frac{d\ \rho_i/\rho_{oi}}{d\theta}\right) = \ell n\ B_i + \frac{E_{ai}}{R}\left(\frac{1}{T}\right) + \psi_i\ \ell n\left(\frac{\rho_i - \rho_{ri}}{\rho_{oi}}\right) \tag{5-2}$$

The bracketed terms in Equation (5-2) can be obtained from TGA data. As the number of data points is larger than three, the equations will overdetermine the values of kinetic constants. Hence, an optimum curve fitting procedure is required. If we write Equation (5-2) in matrix notation, it has the form

$$B = AX \tag{5-3}$$

where B and A are matrices whose elements are determined from the TGA data and X is the matrix of best fit parameters. The curve fitting procedure is then applied by multiplying Equation (5-3) by the transpose of A

$$A^T B = A^T A X \tag{5-4}$$

where $A^T A$ is square and determinate. Hence, the X matrix can be evaluated by Gaussian elimination from the transformed normal equations.

The experimental data used for data reduction are obtained from thermogravimetric analysis (TGA). TGA is an experimental procedure to measure the pyrolysis mass loss history at a prescribed heating rate. The heating agent is usually an inert gas such as argon or nitrogen in order to prevent any surface chemical reaction. Heating rates may range from 0.1°C to 100°C per minute. For the

low cost materials, a heating rate of 10°C per minute was used to obtain TGA data since the higher the heating rate, the lower the accuracy of the data. 10°C per minute is a value that has yielded reliable data in the past. In addition, the pyrolysis kinetics of charring materials behave almost linearly with respect to heating rate. The experimental data was obtained by a subcontract to The Boeing Company.

The kinetic constants which were determined for the low cost materials are presented in Table 5-1. Equation (5-1) was integrated to reproduce TGA results. Excellent agreement was achieved which indicates the quality of the correlated kinetic constants (see Figures 5-1 to 5-5).

5.2 ELEMENTAL COMPOSITION

The elemental composition of the pyrolysis gas and char must be known in order to generate surface thermochemistry tables and determine the pyrolysis gas enthalpy. The char composition for canvas and carbon phenolic materials is often easy to determine as it is merely carbon residue. To determine the pyrolysis gas composition, however, requires a knowledge of both the virgin material composition and the residual mass fraction. The virgin material composition is usually provided by the manufacturers, and the residual mass fraction is known from TGA. With this information, the elemental composition of pyrolysis gas can then be evaluated by the following equations:

$$K_{py_i} = \frac{K_{v_i}}{1 - r} \tag{5-5}$$

$$K_{py_c} = \frac{K_{v_c} - r}{1 - r} \tag{5-6}$$

where K is the mass fraction; r is the residual mass fraction; and subscripts py, c, v denote pyrolysis gas, carbon, and virgin material, respectively.

The evaluated pyrolysis gas elemental compositions of the low cost materials are presented in Table 5-2.

5.3 HEAT OF FORMATION

The virgin material heat of formation is determined from

$$\Delta H_{f_{virgin}} = r\left(\Delta H_{f_{resin}}\right) + \left(1 - r\right)\left(\Delta H_{f_{reinf}}\right) \tag{5-7}$$

TABLE 5-1. DECOMPOSITION KINETICS OF LOW COST MATERIALS

Material	Reaction No. i	ρ_{o_i} (lbm/ft^3)	ρ_{r_i} (lbm/ft^3)	B_i (sec^{-1})	ψ_i	E_{ai}/R (°R)	Γ
FM5790	1	2.375	0	4.8	0.358	7787.6	1.0
	2	19.135	75.560	3.5712×10^6	2.259	27825.0	
	3	-	-	-	-	-	
MXG1033F	1	1.0226	0	6.4977×10^4	0.838	12095.0	1.0
	2	101.2374	90.3949	2.09904×10^6	2.667	23372.0	
	3	-	-	-	-	-	
4K9502	1	6.622	0	5.9285×10^2	1.091	10096.0	0.5
	2	88.906	0	2.39295×10^{11}	1.317	35602.0	
	3	81.048	51.206	2.37558×10^7	3.101	28225.0	
MXC313P	1	2.4756	0	160.464	2.5591	8302.88	0.5
	2	8.5764	0	4.884×10^9	1.2265	35541.80	
	3	165.7818	143.2356	1.70007×10^{22}	6.9232	64876.00	
4CSP08	1	1.8965	0	0.77715	0.91273	5522.17	1.0
	2	79.6735	67.4994	7.791	0.96349	13005.18	
	3	-	-	-	-	-	

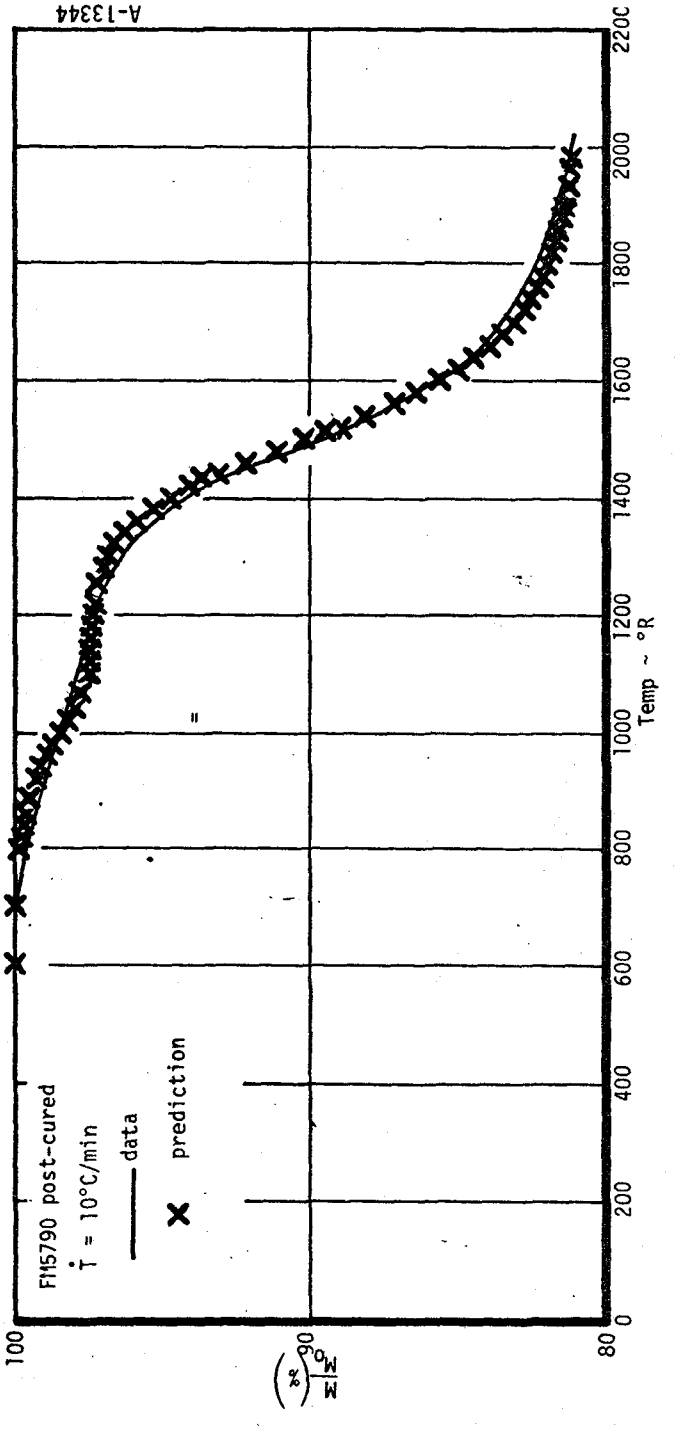

Figure 5-1. Comparison of TGA data and CMA prediction.

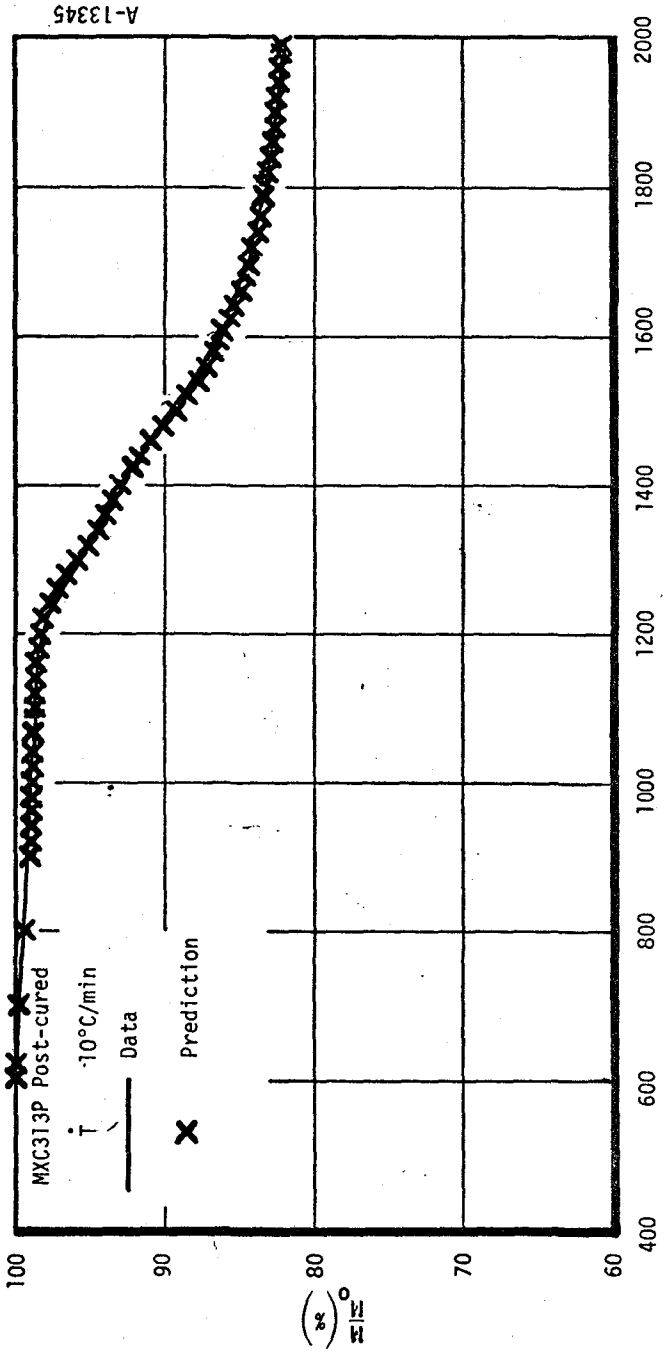

Figure 5-2. Comparison of TGA data and CMA prediction.

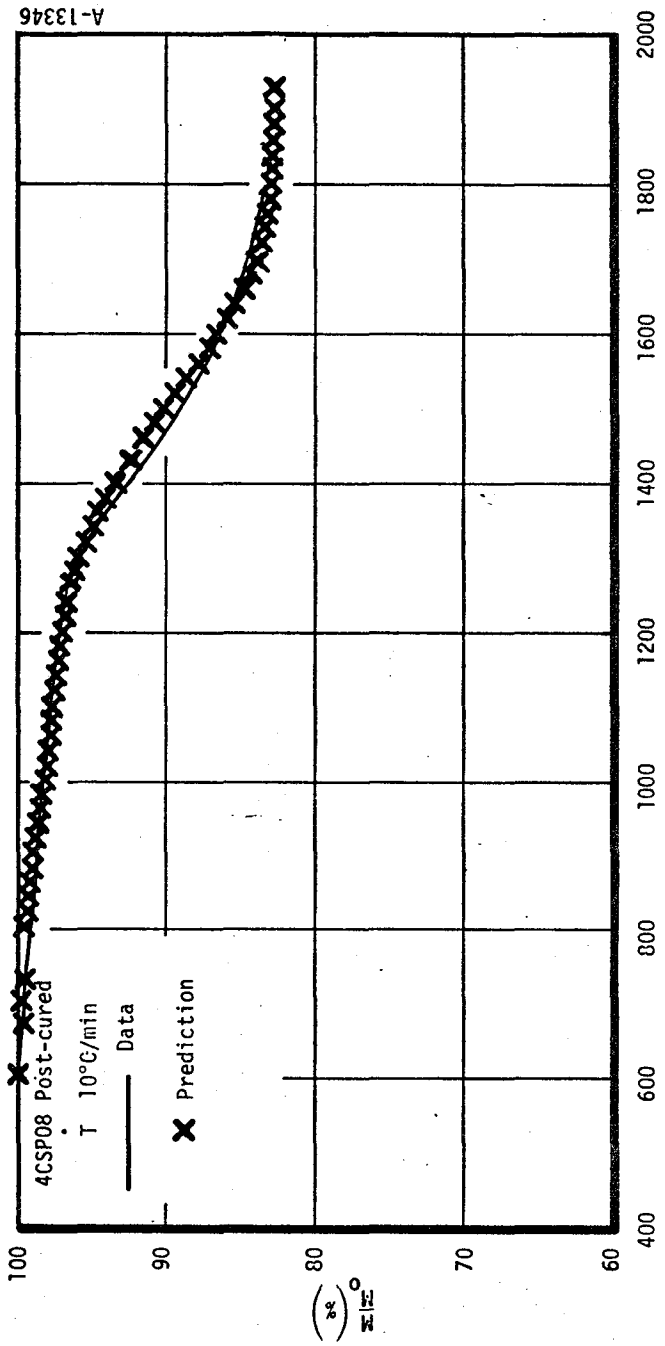

Figure 5-3. Comparison of TGA data and CMA prediction.

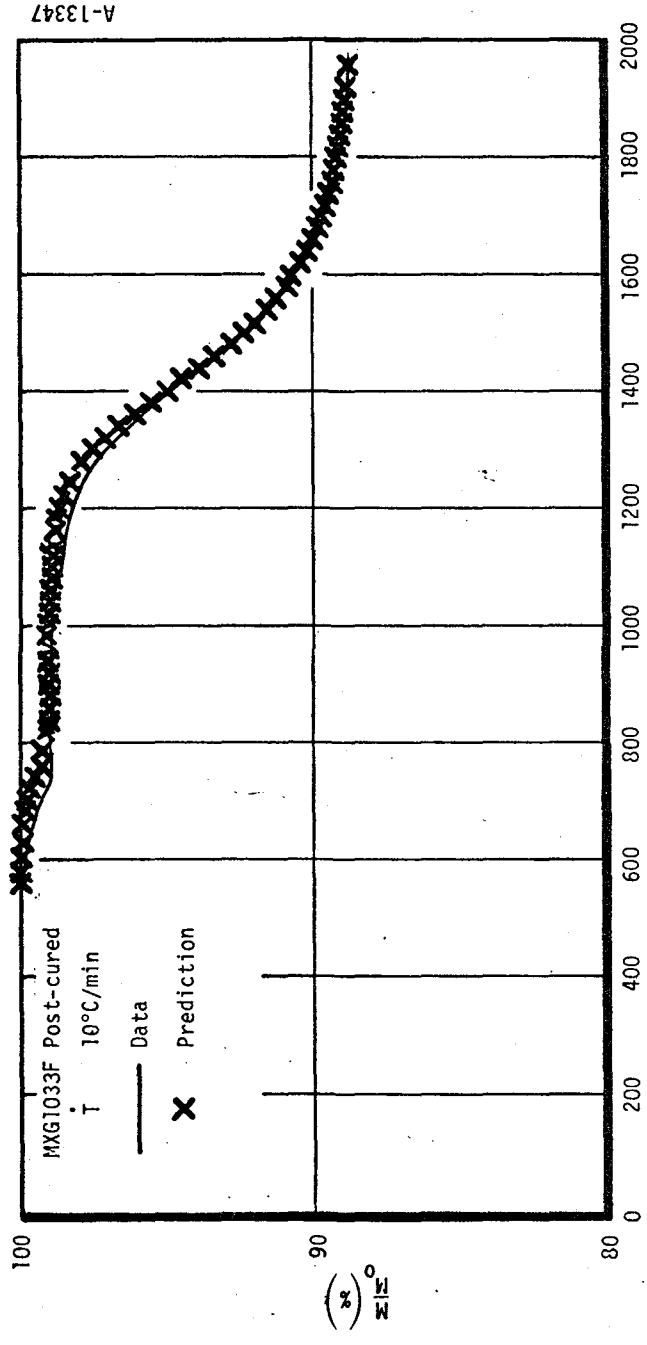

Figure 5-4. Comparison of TGA data and CMA prediction.

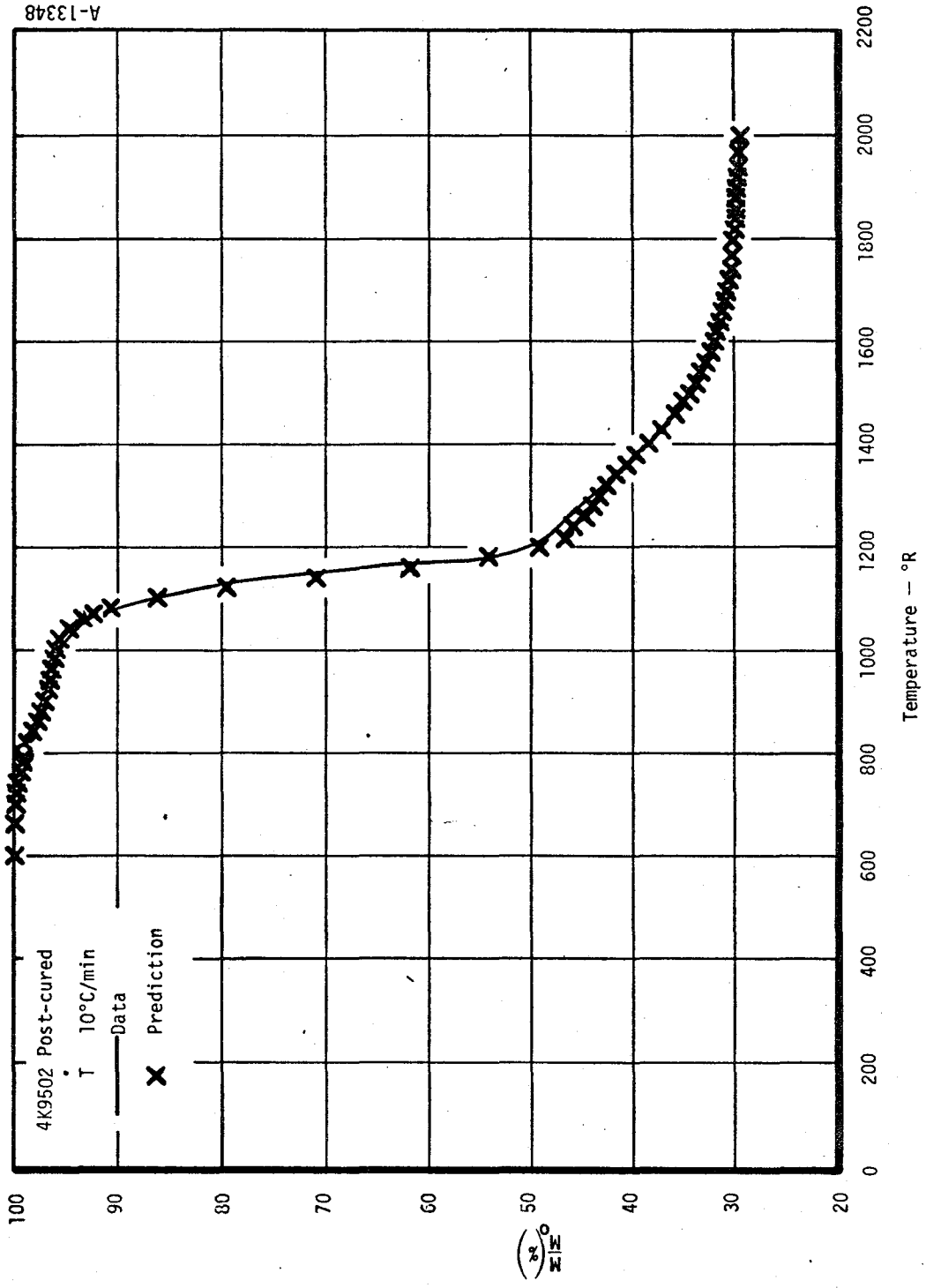

Figure 5-5. Comparison of TGA data and CMA prediction.

TABLE 5-2. ELEMENTAL COMPOSITION OF PYROLYSIS GAS

Type of Material	Mass Fraction		
	H	C	O
FM5790	0.14727	0.46301	0.38972
MXG1033F	0.19383	0.29337	0.51280
4CSP08	0.16766	0.38884	0.44350
MXC313P	0.13526	0.50679	0.35795
4K9502	0.08880	0.40760	0.50360

The reinforcement material for the five selected low cost materials is either carbon or canvas. The nominal values for resin and reinforcement heats of formation are shown in Table 5-3. For the

TABLE 5-3. NOMINAL VALUES FOR RESIN AND REINFORCEMENT HEATS OF FORMATION

$\Delta H_{f_{C_2H_2O}}$	-1083 Btu/lbm
$\Delta H_{f_{canvas}}$	-2569 Btu/lbm
$\Delta H_{f_{carbon}}$	0 Btu/lbm

char, the heat of formation again is just merely the carbon heat of formation, i.e., zero.

Table 5-4 presents the evaluated heats of formation of the virgin low cost materials.

TABLE 5-4. HEAT OF FORMATION OF VIRGIN LOW COST MATERIALS

Type of Material	ΔH_f (Btu/lbm)
4CSP08	- 487.35
FM5790	- 476.52
MXG1033F	- 379.05
MXC313P	- 433.20
4K9502	-1944.88

5.4 DENSITY

The virgin material density was determined by precise weight and dimension measurement of samples which have regular geometric shapes. The char density is evaluated by multiplying the virgin material density by the residual mass fraction which was obtained from the TGA data.

The measured or evaluated densities are shown in Table 5-5.

TABLE 5-5. DENSITIES OF LOW COST MATERIALS

Materials	Virgin Density (lbm/ft^3)	Char Density (lbm/ft^3)
4CSP08	81.570	67.500
FM5790	93.510	75.560
MXG1033F	102.260	90.395
MXC313P	88.417	71.6178
4K9502	88.288	25.603

5.5 SPECIFIC HEAT CAPACITY

The specific heat of the virgin material was determined by graphical differentiation of specific enthalpy versus temperature curves. The enthalpy was measured using an ice mantle calorimeter. The calorimeter consists of a copper well, a distilled water vessel surrounding the copper well, an ice bath surrounding the vessel, and an insulation filled container surrounding the ice bath. An ice mantle is formed on the outer surface of the copper well.

The material sample is heated to the desired uniform temperature in a muffle furnace and then dropped directly from the furnace into the calorimeter. The energy lost by the sample as it cools results in a volume change in the distilled water due to the partial melting of the ice mantle. This volume change is quantitatively related to the original energy of the sample. A small leak inherent in the apparatus is calibrated after each test and accounted for in the data reduction. The samples used in the calorimeter tests are approximately 0.02 cubic inch in volume.

Table 5-6 shows the evaluated virgin material specific heat as a function of temperature. The char specific heat, however, need not be determined since the specific heat capacity of carbon is known.

5.6 THERMAL CONDUCTIVITY

The material thermal conductivity was determined by two separate techniques. The applicability of each technique is dependent on the temperature and state of the material. The conventional technique is applicable for the virgin material over the temperature range from room temperature to approximately 700°F. The dynamic technique is applicable for the virgin, partially charred, or fully charred material over the temperature range from 700°F to approximately 4000°F.

TABLE 5-6. VIRGIN MATERIAL SPECIFIC HEAT CAPACITY

Materials	Temperature (°R)	Cp (Btu/lbm-°R)
4K9502	500	0.360
	800	0.440
	1000	0.500
	1200	0.540
	2000	0.540
	6000	0.540
4CSP08	500	0.200
	800	0.320
	1000	0.400
	1200	0.460
	1400	0.500
	2000	0.500
	6000	0.500
MXG1033F	500	0.120
	800	0.320
	1000	0.380
	1200	0.430
	1400	0.440
	2000	0.440
	6000	0.440
MXC313P	500	0.160
	800	0.340
	1000	0.380
	1200	0.420
	1400	0.440
	2000	0.440
	6000	0.440
FM5790	500	0.160
	800	0.360
	1000	0.420
	1200	0.420
	1400	0.420
	2000	0.420
	6000	0.420

5.6.1 Virgin Material Thermal Conductivity

Virgin material thermal conductivity was determined using a small thermal conductivity cell. In this apparatus, the testing sample (1/6" thick wafer) is sandwiched between an aluminum block (0.75 x 1.25 x 1.50 inches), and an aluminum slab (0.25 x 1.25 x 1.50 inches). The temperature difference (ΔT) is then measured across the testing sample as the block is heated at a linear rate equal to 4°C/min.

For calibration, an aluminum wafer is placed in the cell. The resulting ΔT is assumed to be the temperature baseline. A wafer of fused silica is run as a reference sample, and an instrument constant is calculated for each 100° interval. The comparative values are then calculated from the expression:

$$k = \frac{CL^2}{\Delta T} \tag{5-8}$$

where k is the thermal conductivity, C is the instrument constant, L is the wafer thickness, and ΔT is the temperature difference across the wafer.

Figures 5-6 to 5-10 present the measured thermal conductivity at both 0° and 90° orientation for the virgin materials.

5.6.2 Dynamic Thermal Conductivity

The dynamic thermal conductivity technique is a combined experimental and analytical technique which has the inherent advantage that the char characteristics of the materials are accurately duplicated. This technique has been described in detail in References 2 through 5, and thus, will only be summarized in the paragraphs below.

The analysis portion of this procedure involves solving the governing equation for transient one-dimensional heat conduction in a charring ablating material. Incorporated within this equation is the model for defining the thermal conductivity of the partially-charred and fully-charred materials. This model is represented by the equation

$$k = (1 - \chi)\, k_p + \chi k_v \tag{5-9}$$

where χ is the mass fraction of virgin material and k_p and k_v are the thermal conductivities for virgin and charred materials, respectively.

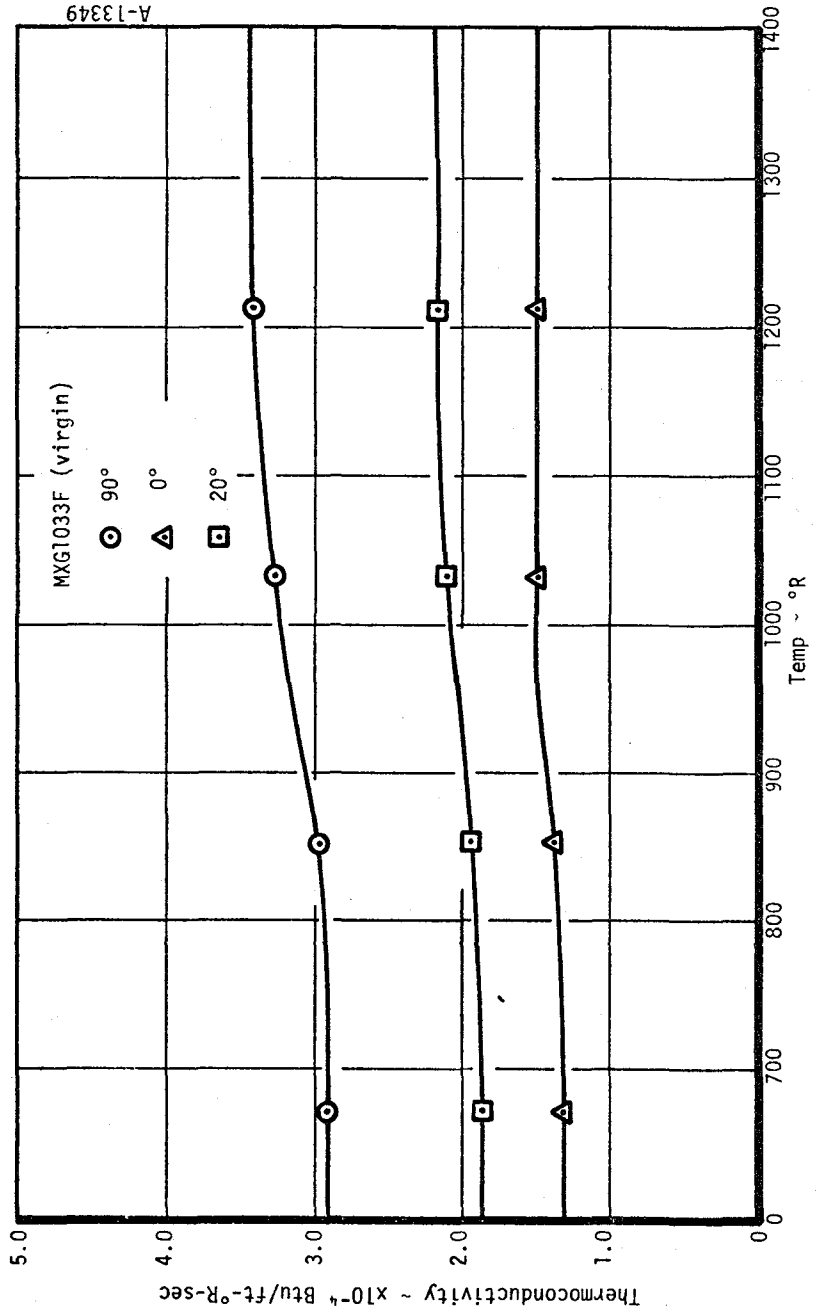

Figure 5-6. Measured virgin material thermal conductivity.

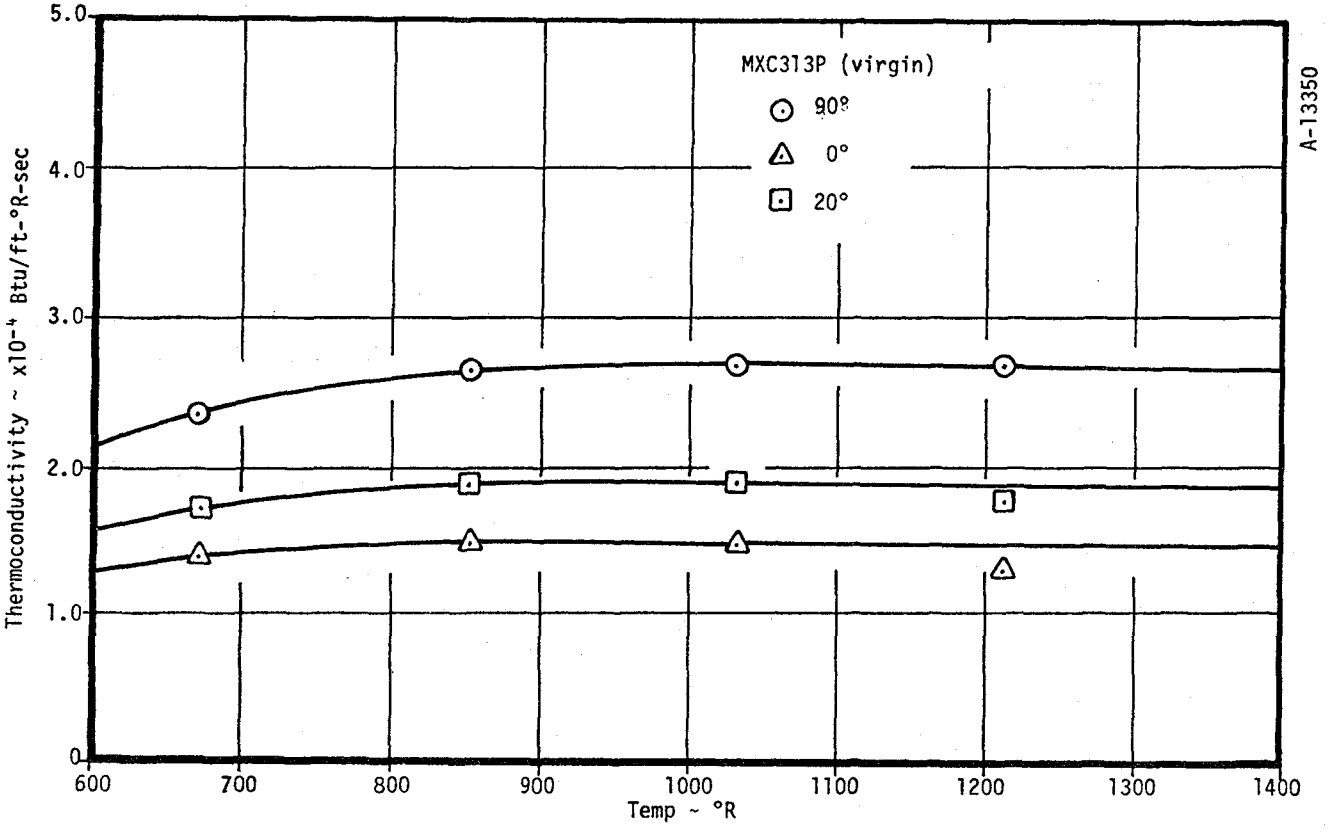

Figure 5-7. Measured virgin material thermal conductivity.

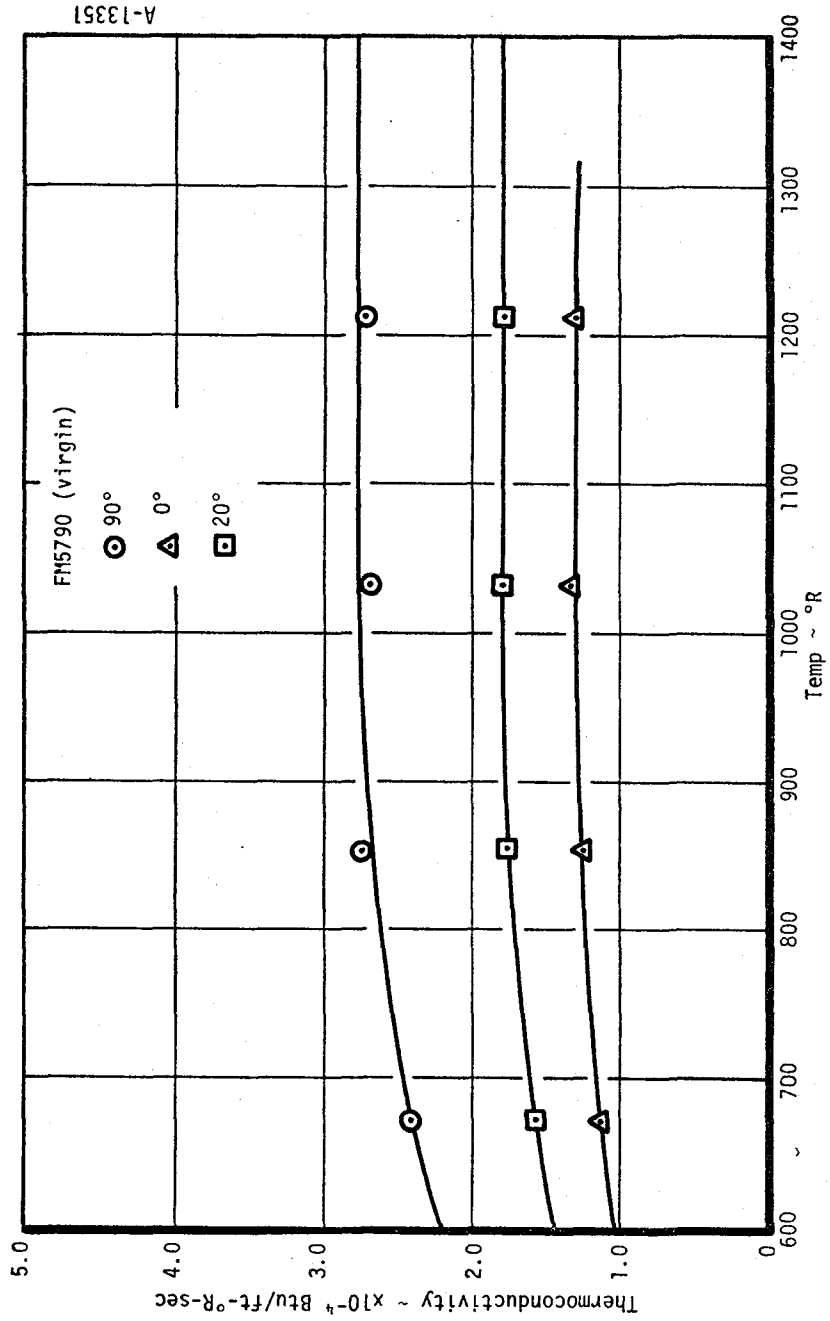

Figure 5-8. Measured virgin material thermal conductivity.

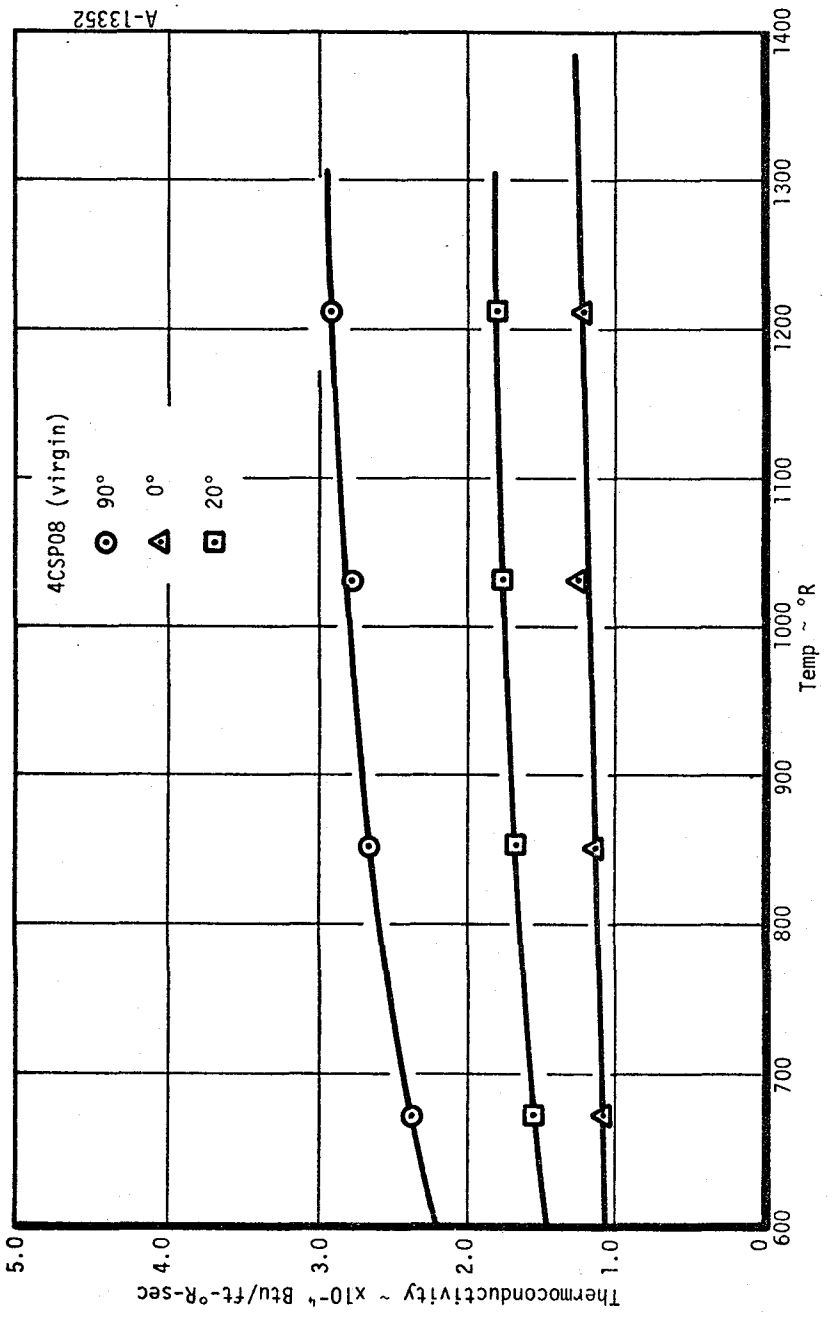

Figure 5-9. Measured virgin material thermal conductivity.

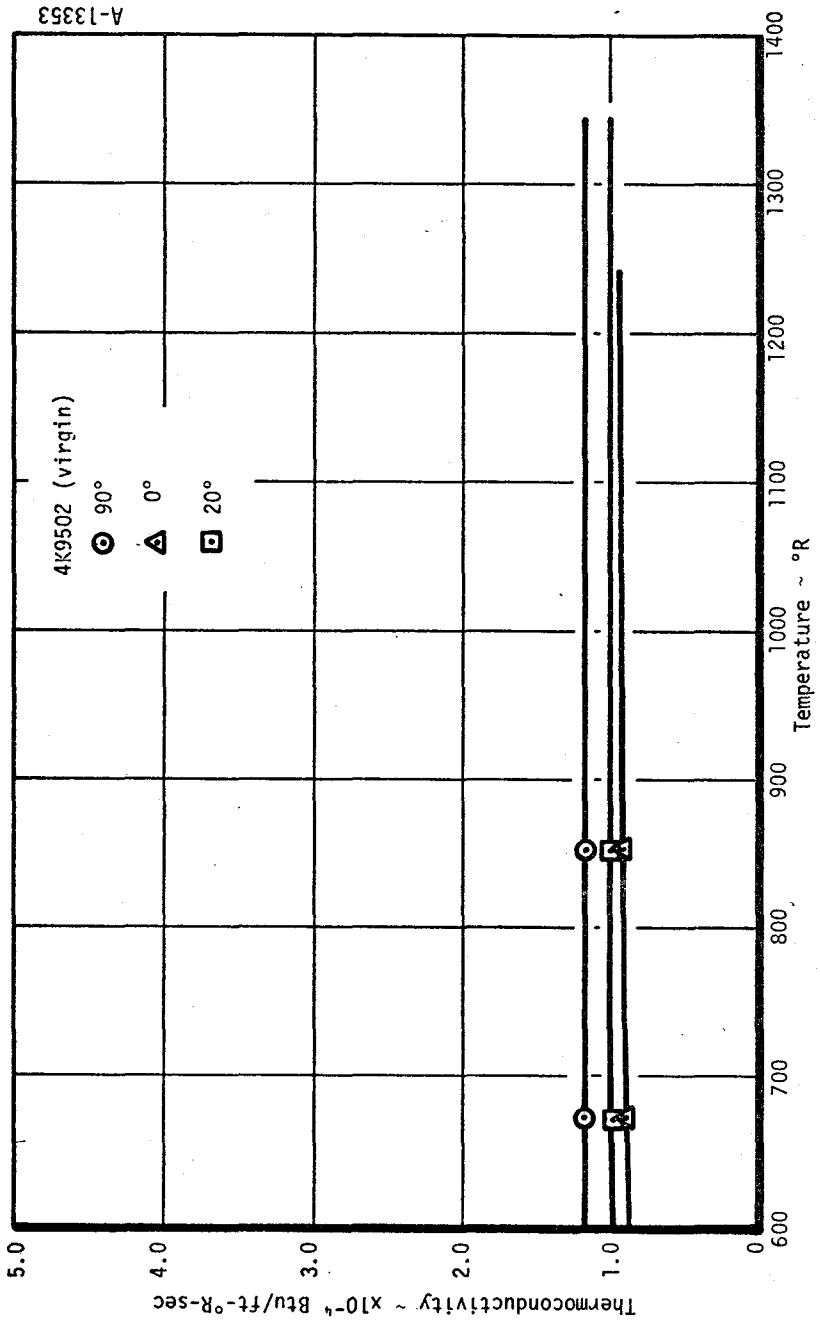

Figure 5-10. Measured virgin material thermal conductivity.

The analytical procedure for defining the thermal conductivity of in-depth charring materials involves solving the governing one-dimentional conservation of energy and mass equations for an impressed surface boundary condition. The flux terms considered in these equations are illustrated in Figure 5-11.

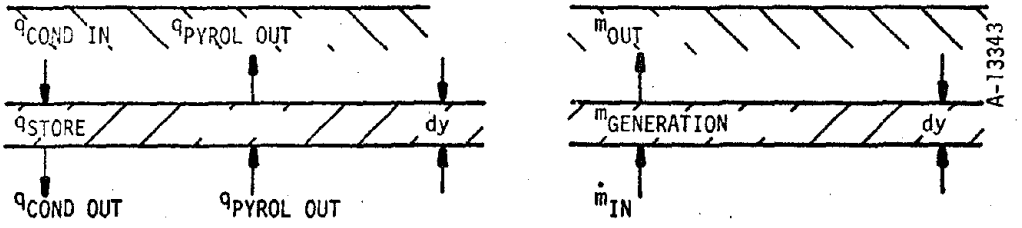

Figure 5-11. Control volumes for in-depth energy and mass balances.

If it is assumed that the pyrolysis gases do not react chemically with the char and the pyrolysis gases pass immediately out through the char, then the conservation of energy equation becomes

$$\frac{\partial}{\partial t}(\rho h A)_y = \frac{\partial}{\partial y}\left(KA\frac{\partial T}{\partial y}\right)_t + \frac{\partial}{\partial y}\left(\dot{m}_g h_g\right)_t \qquad (5\text{-}10)$$

where

A – area

h – total material enthalpy (chemical plus sensible)

h_g – total pyrolysis gas enthalpy

$\dot{m}_g$ – pyrolysis gas flowrate

t – time

T – temperature

y – distance from surface

ρ – density

and the conservation of mass equation becomes

$$\left(\frac{\partial \dot{m}_g}{\partial y}\right)_t = A\left(\frac{\partial \rho}{\partial t}\right)_y \qquad (5\text{-}11)$$

The first term in Equation (5-10) accounts for the change in energy stored within the element, the second term accounts for the net thermal heat conduction across the element, and the third term accounts for the net transfer of thermal energy due to the flow of pyrolysis gases. Equation (5-11) describes the degradation of the material. The decomposition rate $(\partial\rho/\partial t)_y$ is defined as an Arrhenius type expression of the form

$$\left.\frac{\partial\rho}{\partial t}\right)_y = -\sum_{i=1}^{3} B_i e^{-E_{ai}/RT} \rho_{pi} \left(\frac{\rho_i - \rho_{ci}}{\rho_{pi}}\right)^{\psi_i} \qquad (5\text{-}12)$$

where

B — pre-exponental factor

E_a — activation energy

R — gas constant

ρ_p — original density

ρ_c — residual density

ψ — density factor exponent

For most materials, it is sufficient to consider three different decomposing constituents, two describing the resin and one describing the reinforcement. Equations (5-10) through (5-12) are solved by the CMA program which is described in detail in Reference 1.

If the following material thermal and chemical properties are known

- Virgin and char specific heat
- Virgin thermal conductivity
- Virgin and char density
- Resin mass fraction
- Virgin and char heat of formation
- Decomposition kinetics of the resin system

then Equations (5-10) through (5-12) can be solved for the thermal conductivity by using measured in-depth and surface transient temperatures. The method for obtaining the in-depth and surface temperatures is described in the following paragraphs.

The thermal conductivity test samples were tested in the Aerotherm 1 MW APG. The APG is shown schematically in Figure 5-12. The test gases and test conditions were chosen to yield a material thermal response typical of that in the actual application of interest. In addition, chemically inert test gases were used so that the surface recession due to chemical corrosivity is zero. Therefore, this surface boundary condition which is required in the data reduction process was accurately known. The selected test gas, which is shown below, is chemically inert to most materials at high temperatures and also approximates the specific heat capacity of rocket motor combustion products (Reference 2).

Species	Mass Fraction
H_e	0.2236
N_2	0.7764

The test configuration used was a two-dimensional (2-D) supersonic nozzle in which the conductivity test section formed one wall as shown in Figure 5-13. The measurement station was the nozzle throat which is of finite length and yields a significant region of well-defined, constant test conditions. The 2-D configuration allowed the test section to be obtained from parts fabricated by representative techniques (e.g., tape wrapped at any layup angle), allowed an accurate thermocouple instrumentation technique, and provided an approximately one-dimensional heat flux path.

The surface temperature boundary condition was measured continuously during each test with an infrared optical pyrometer. The in-depth temperatures were measured continuously during each test at four locations and, together with the measured surface recession and surface temperature, provided the test results on which the calculation of thermal conductivity was based. Tungsten-5 percent rhenium thermocouples were used for temperature measurements at the two locations nearest the surface. Chromel/alumel thermocouples were used at the other locations. The thermocouple installation technique is illustrated in Figure 5-13. The stepped hole which accepts the thermocouple provides intimate contact with the material. The thermocouple wires were brought down the side walls through alumina sleeving to prevent shorting across the electrically conductive char and/or virgin material. The thermocouple wire size, compatible with the capabilities of thermocouple hole drilling, was 0.005 inch. The nominal thermocouple depths were 0.075, 0.150, 0.250, and 0.400. The actual thermocouple depths were accurately determined from x-ray negatives. The details and techniques for drilling the stepped hole and for thermally instrumenting the model are presented in Reference 3.

Since delamination is likely in 0° orientation testing, this experiment was conducted in the 20° and 90° orientations.

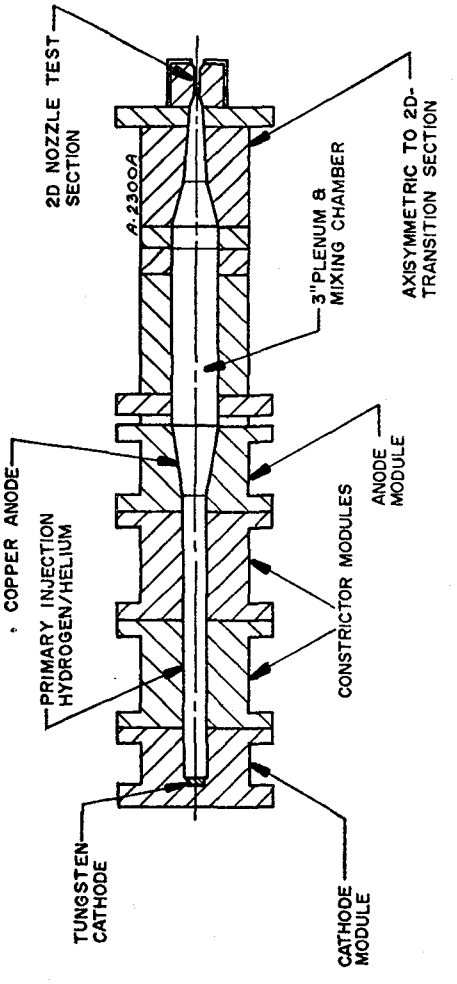

Figure 5-12. Aerotherm constrictor arc, rocket simulator configuration.

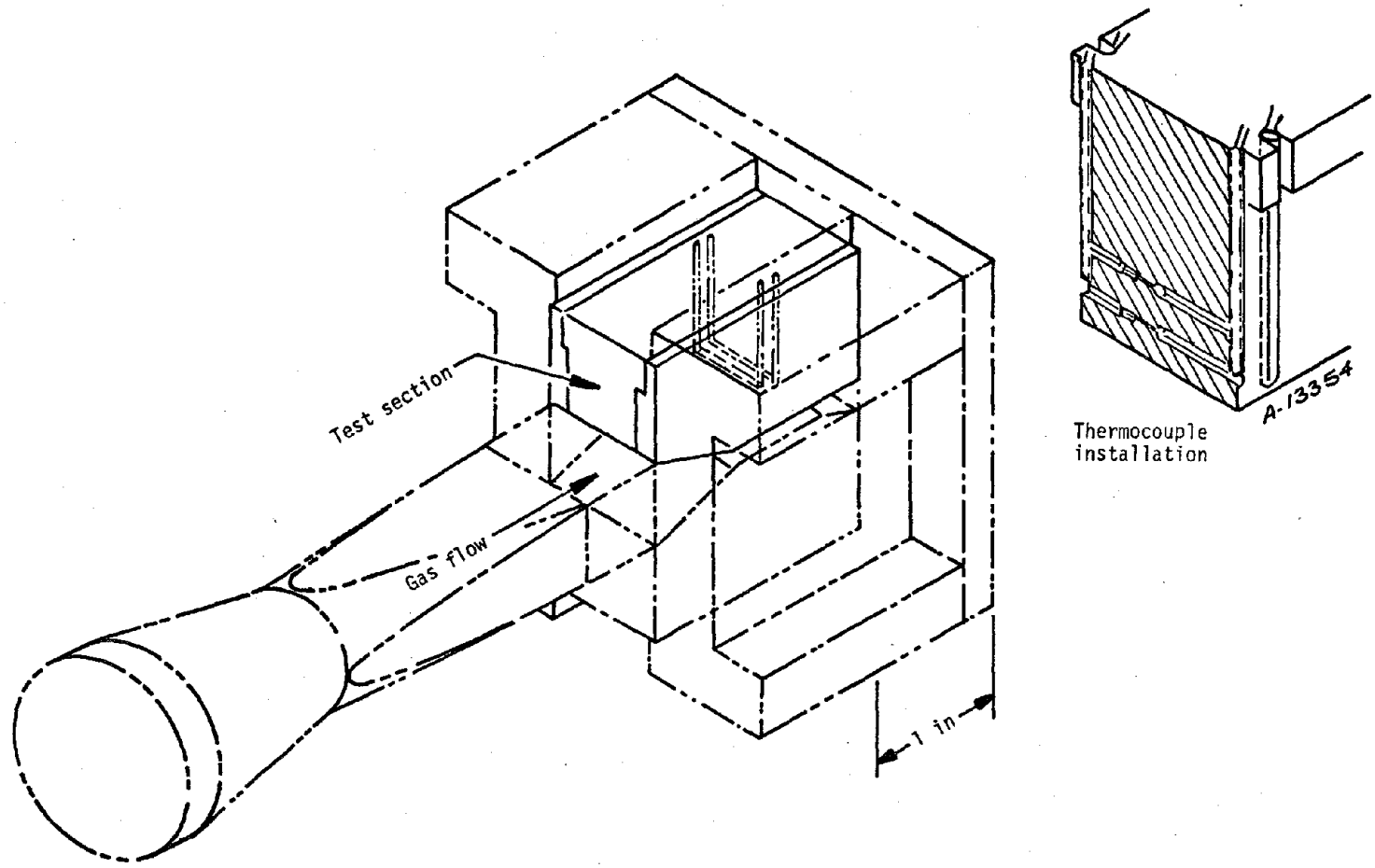

Figure 5-13. Typical instrumented duct flow test section.

The following equation was then applied to back out the 0° orientation conductivity after conductivities in the 20° and 90° orientations were evaluated.

$$k_o = \frac{k_{20°} - k_{90°} \sin 20°}{1 - \sin 20°}$$

The evaluated char conductivities for 0° and 90° orientation are shown in Figures 5-14 and 5-15. The accuracy of the calculated char conductivity can be judged by comparing the calculated and measured in-depth temperature histories (see Figures 5-16 through 5-25). Except for a few anomalies the comparisons are excellent for the first 30 seconds of the tests. Subsequently, the predictions deviate from the measured values. This deviation was due to heat losses to the water cooled APG components so that no attempt was made to match this data.

Post test char depth profiles are shown schematically in Figure 5-26. Differences in char penetration between 20° and 90° orientation are obvious as are the effects of sidewall cooling. The canvas phenolic material exhibited very erratic data and shows a correspondingly poor char profile, especially for the 20° orientation. Of the data presented in Figures 5-14 and 5-15, the canvas phenolic has the lowest confidence level.

The anomalies are due to thermocouple breakage or a separation of the thermocouples from the char. The latter would result in very erratic temperatures which, for instance, were observed for canvas phenolic (4K9502).

5.7 CHARACTERIZATION SUMMARY

The full characterization data is summarized in Tables 5-7 through 5-11. These tables provided the information required for a thermal analysis of low cost materials.

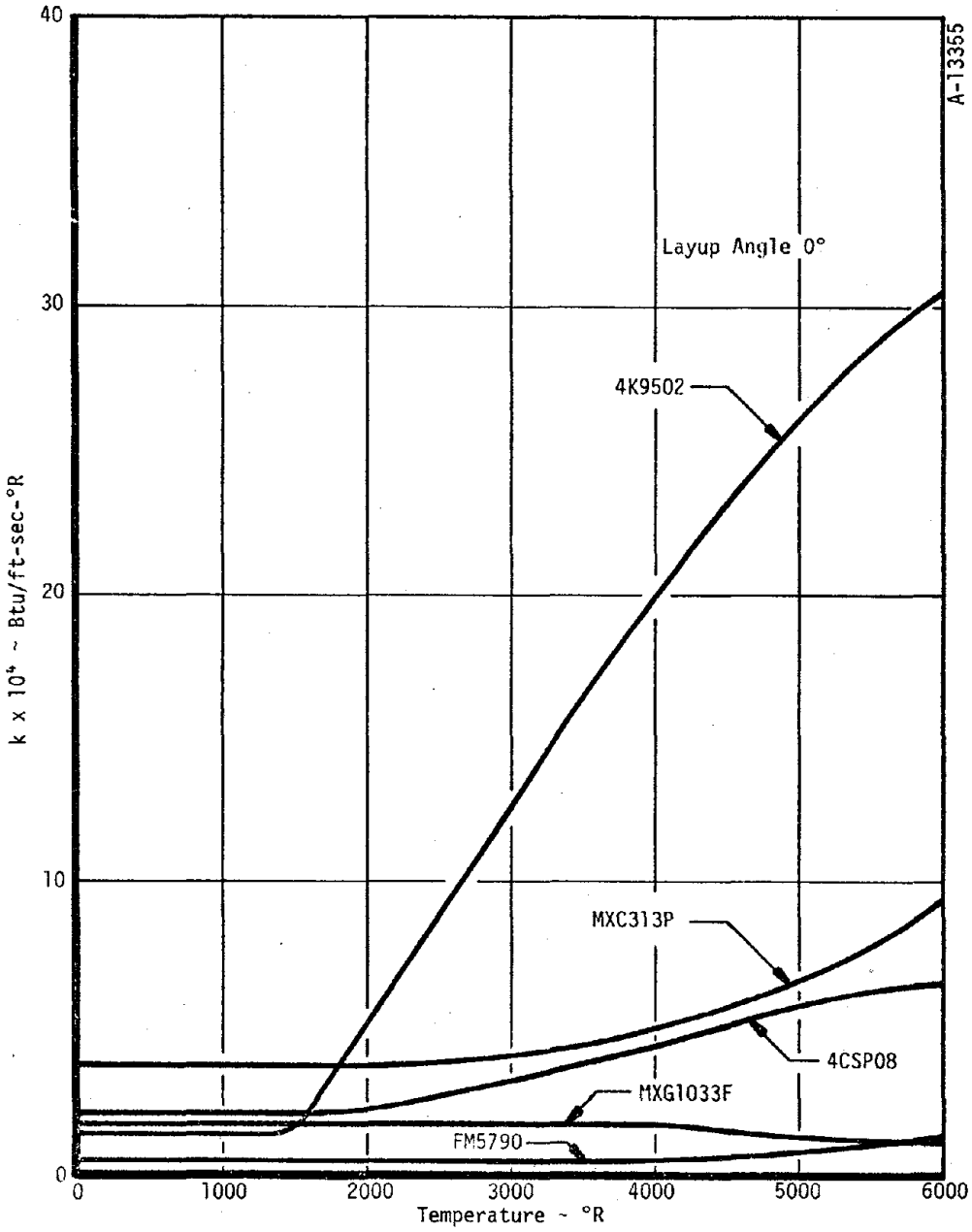

Figure 5-14. 0° char thermal conductivity.

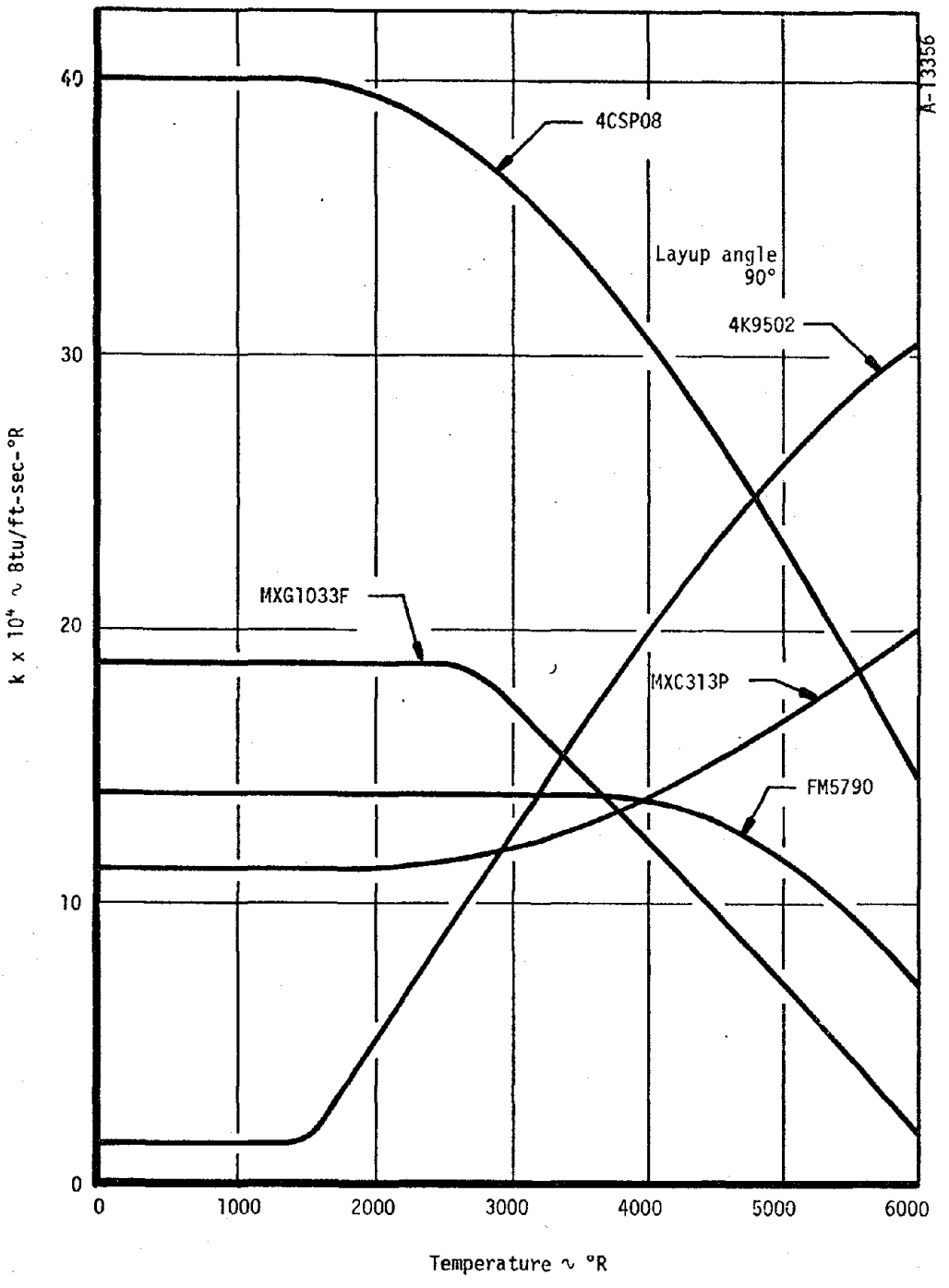

Figure 5-15. 90° char thermal conductivity.

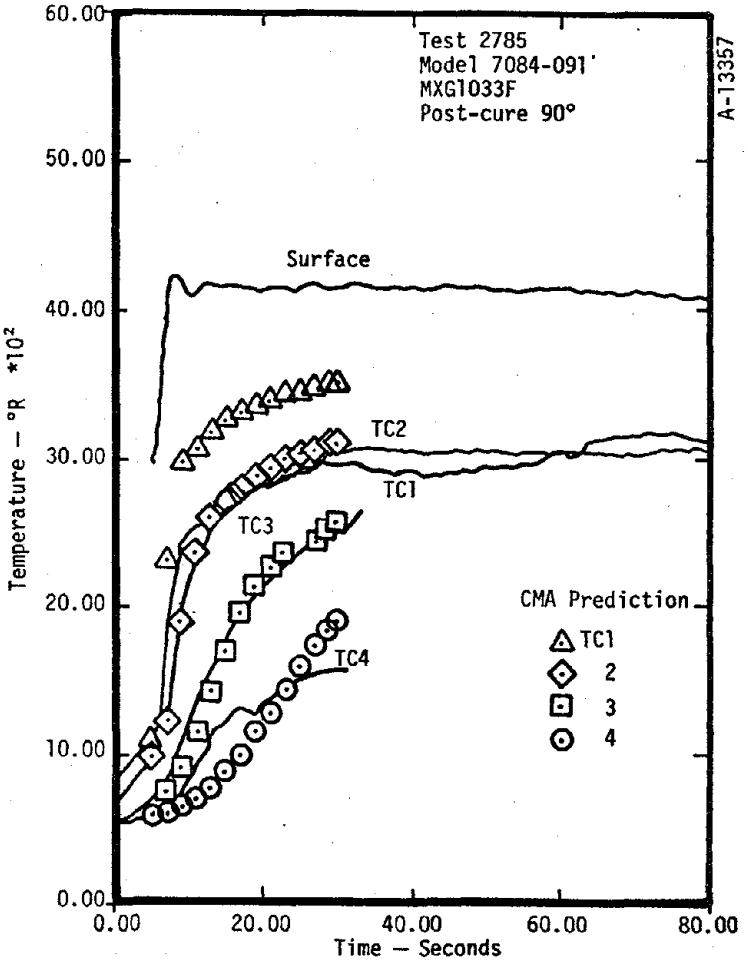

Figure 5-16. Comparison of in-depth thermocouple measurements and CMA prediction.

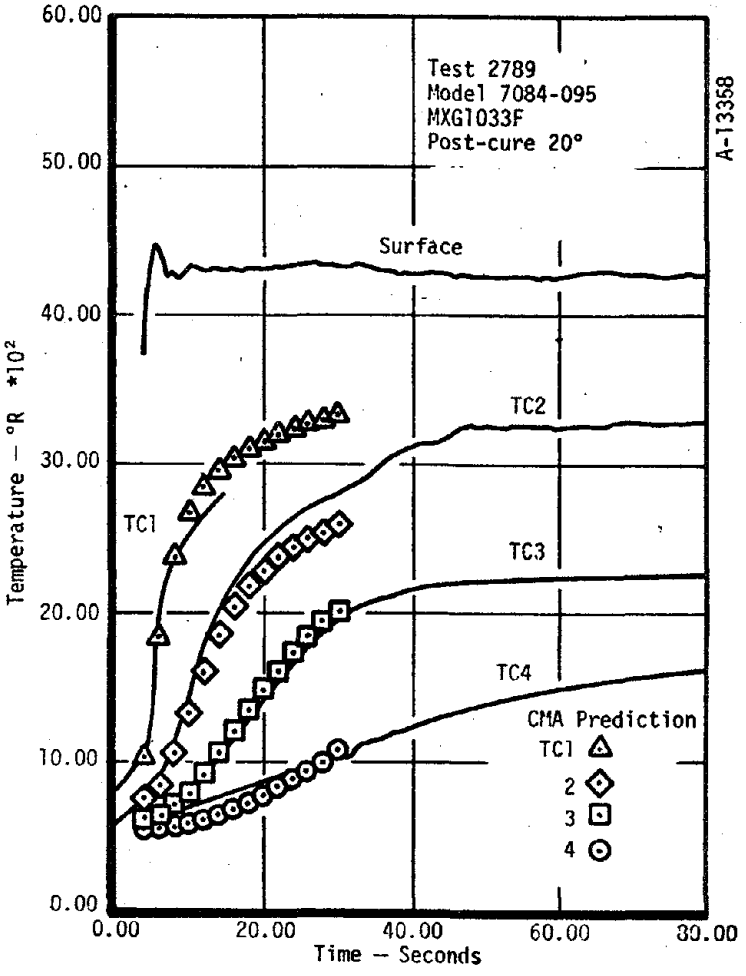

Figure 5-17. Comparison of in-depth thermocouple measurements and CMA prediction.

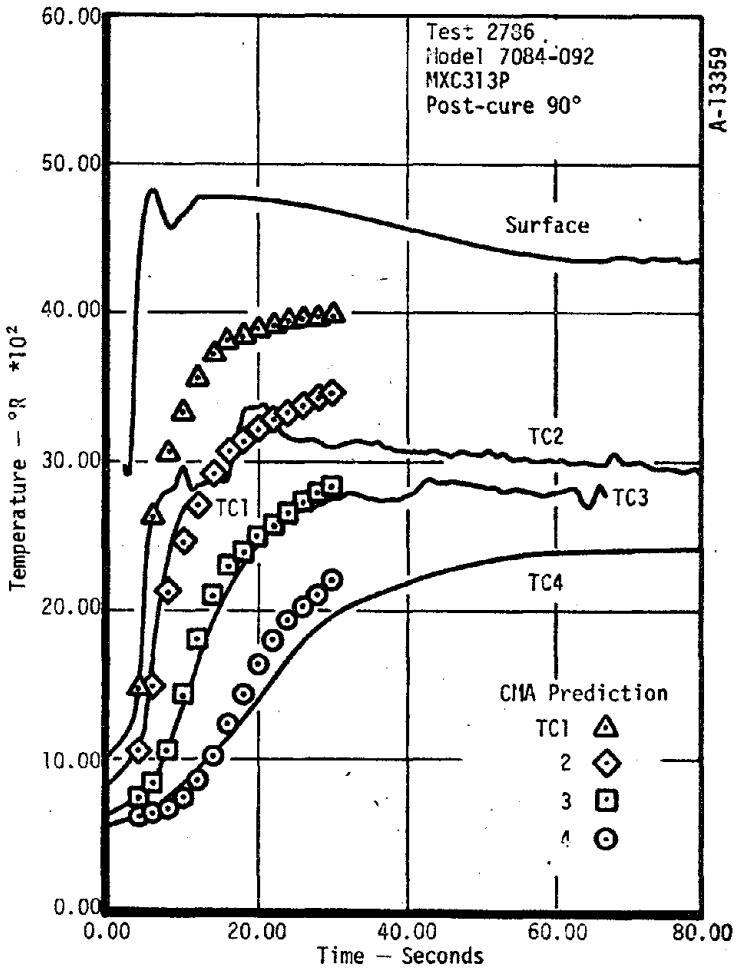

Figure 5-18. Comparison of in-depth thermocouple measurements and CMA prediction.

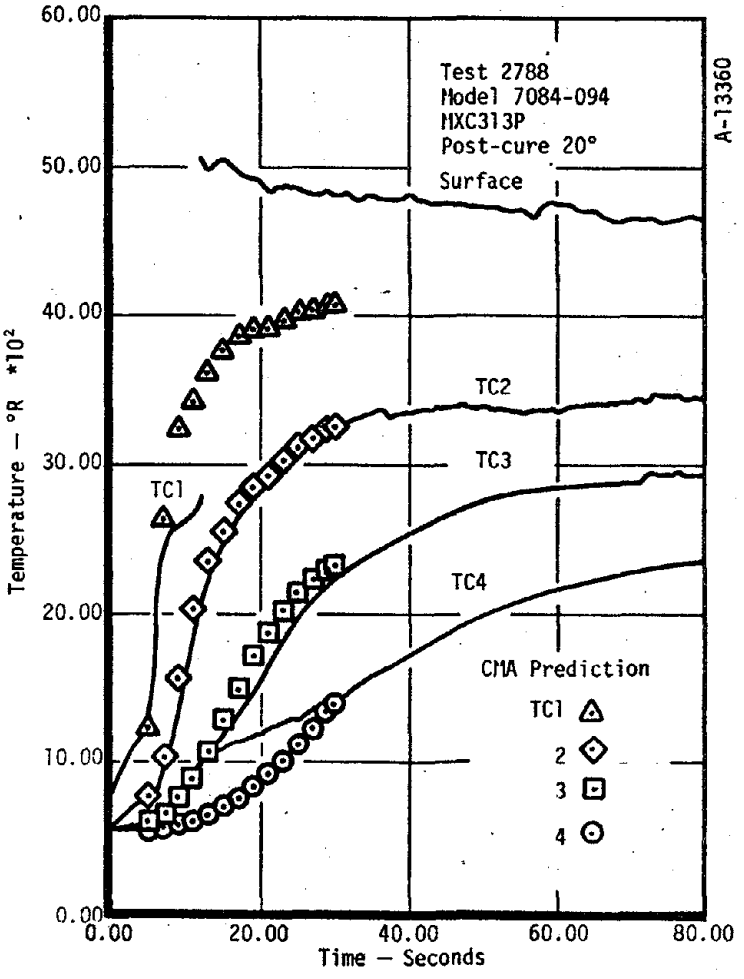

Figure 5-19. Comparison of in-depth thermocouple measurements and CMA prediction.

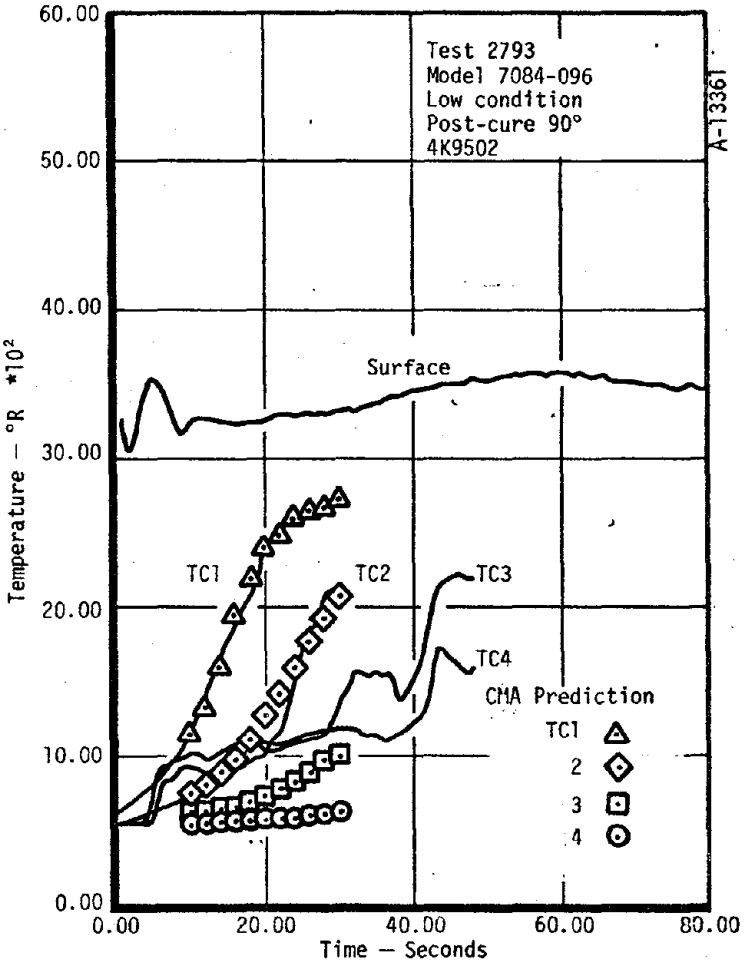

Figure 5-20. Comparison of in-depth thermocouple measurements and CMA prediction.

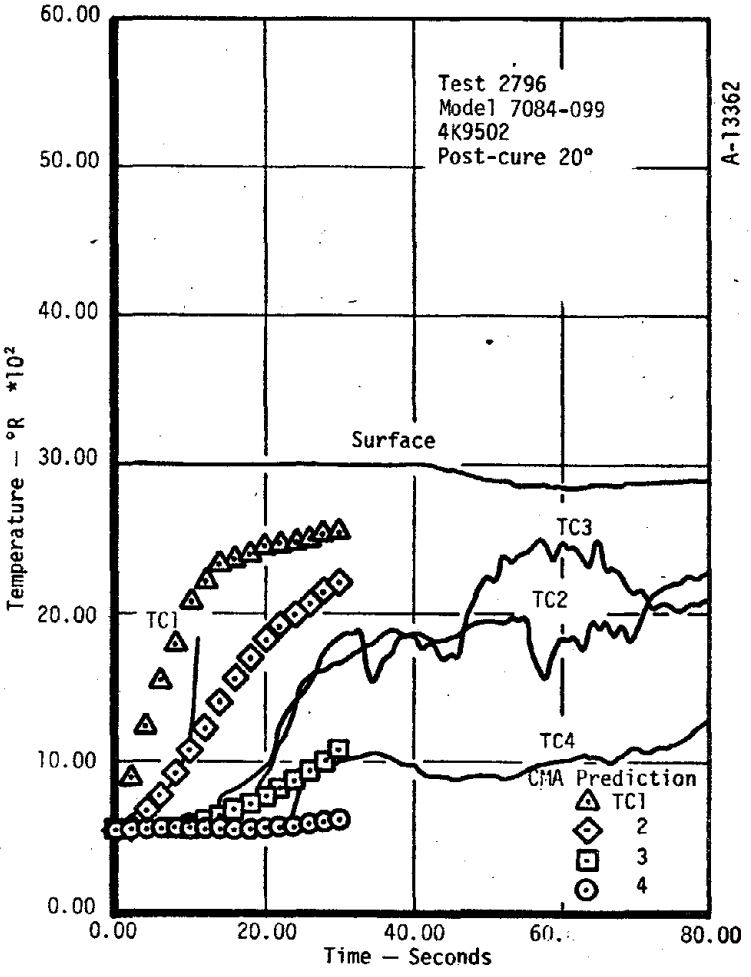

Figure 5-21. Comparison of in-depth thermocouple measurements and CMA prediction.

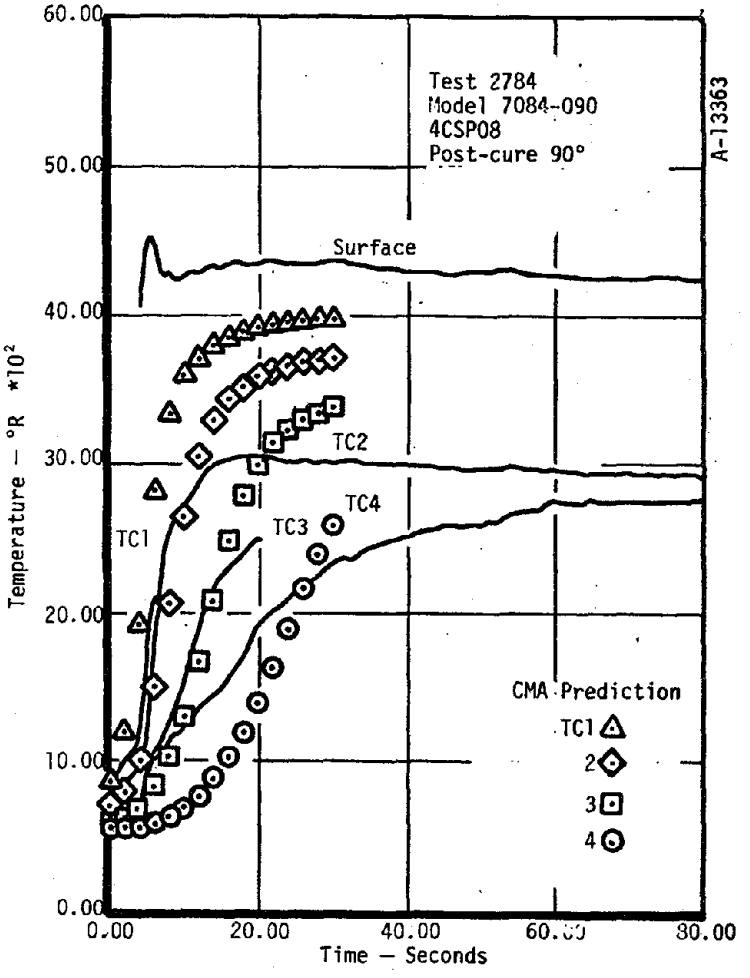

Figure 5-22. Comparison of in-depth thermocouple measurements and CMA prediction.

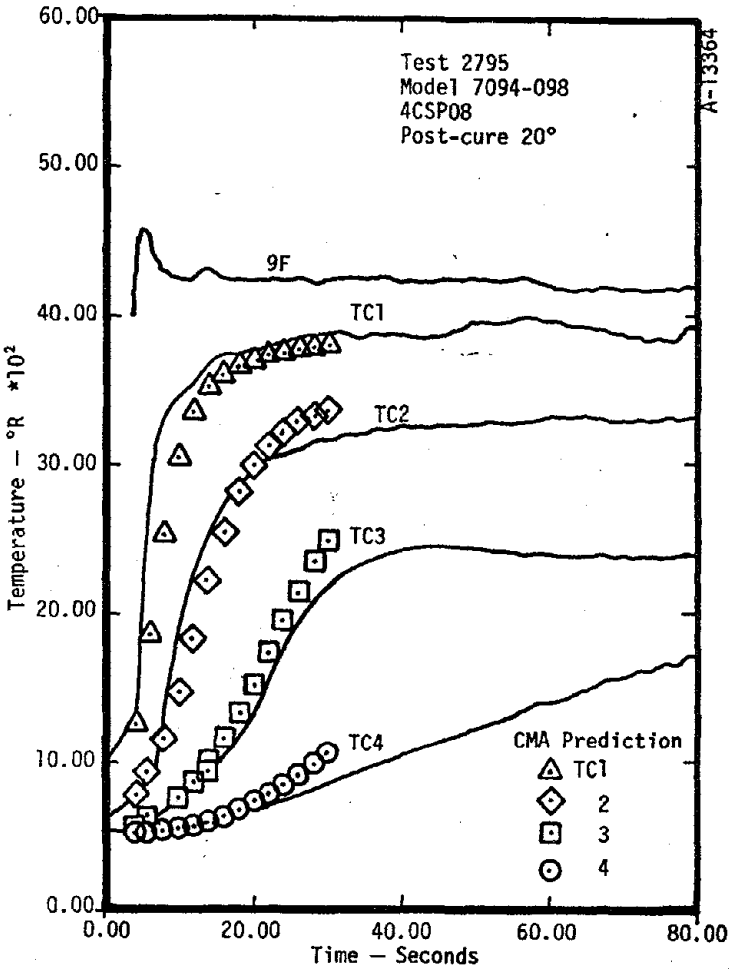

Figure 5-23. Comparison of in-depth thermocouple measurements and CMA prediction.

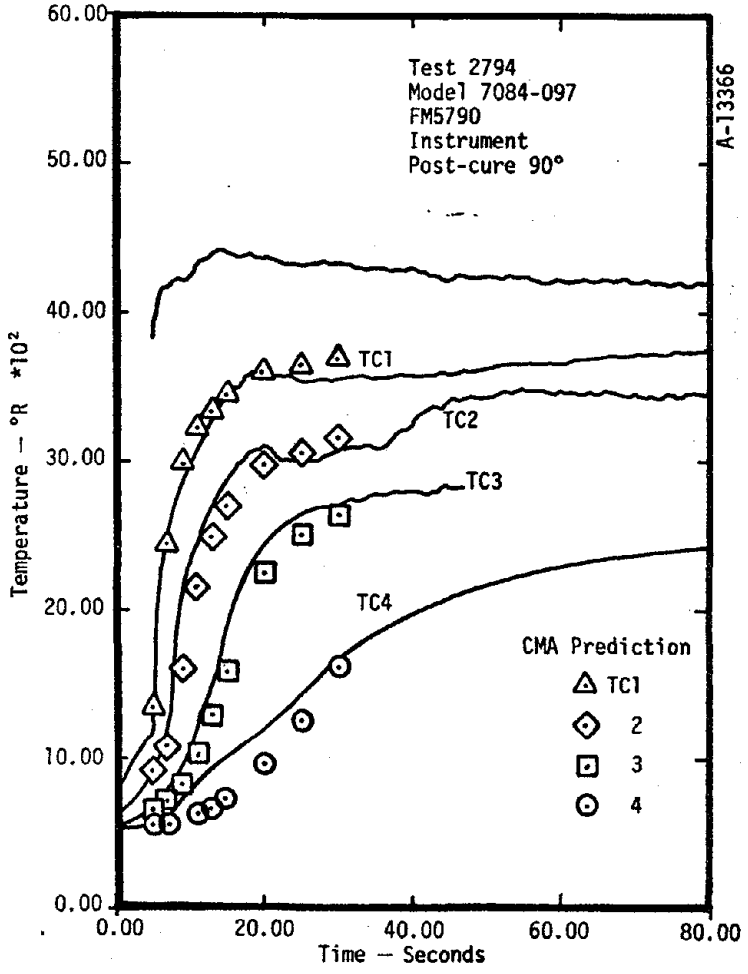

Figure 5-24. Comparison of in-depth thermocouple measurements and CMA prediction.

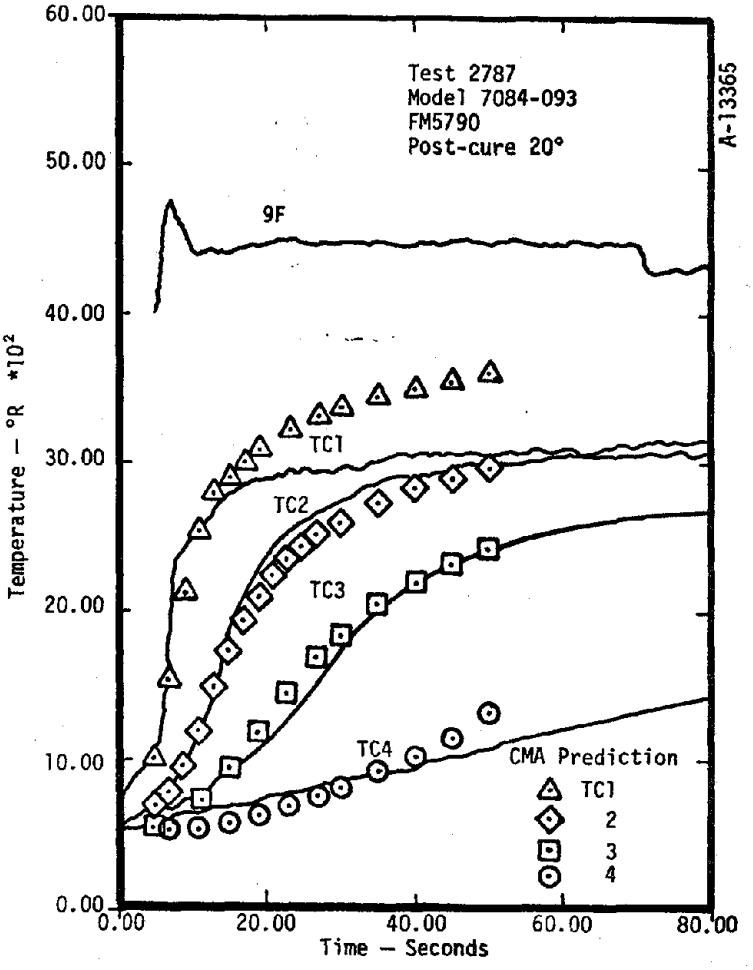

Figure 5-25. Comparison of in-depth thermocouple measurements and CMA prediction.

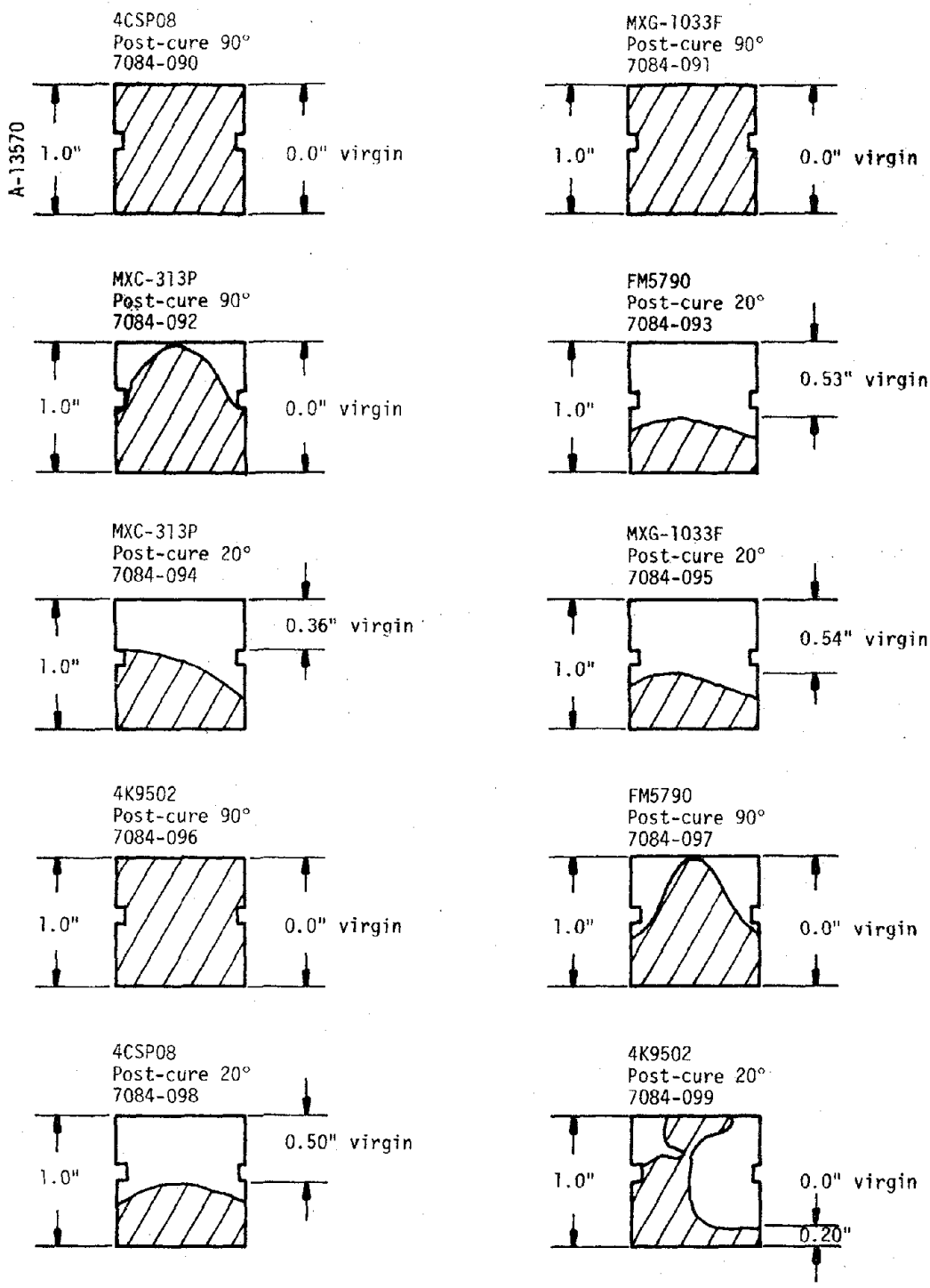

Figure 5-26. Char layer profiles for char conductivity test samples.

TABLE 5-7. THERMAL AND PHYSICAL PROPERTIES OF PITCH MAT CARBON PHENOLIC

Material	Nominal Density (lb/ft³)	Nominal Resin Mass Fraction	Heat of Formation (Btu/lbm)	Resin Elemental Formula (Phenolic)	Reinforcement Elemental Formula	Fail Temperature (°R)	Virgin Material					Char			
							Temperature (°R)	Specific Heat (Btu/lbm-°R)	Thermal Conductivity x10⁴ (Btu/ft-sec-°R) 0° layup	Thermal Conductivity x10⁴ (Btu/ft-sec-°R) 90° layup	Emissivity	Specific Heat (Btu/lbm-°R)	Thermal Conductivity x10⁴ (Btu/ft-sec-°R) 0° layup	Thermal Conductivity x10⁴ (Btu/ft-sec-°R) 90° layup	Emissivity
Pitch Mat Carbon Phenolic 4CSP08	81.570	0.172	-487.35	C_6H_6O	C	–	530	0.200	1.05	2.20	0.85	0.210	2.00	40.00	0.85
							800	0.320	1.12	2.60		–	2.00	40.00	
							1000	0.400	1.16	2.80		0.430	2.00	40.00	
							1200	0.460	1.22	2.91		–	2.00	40.00	
							1400	0.500	1.25	2.95		0.470	2.00	40.00	
							2000	|	|	|		0.484	2.15	39.40	
							3000	|	|	|		0.493	3.10	36.10	
							4000	|	|	|		0.498	4.25	30.50	
							5000	|	|	|		0.500	5.75	23.20	

a) The decomposition kinetic constants for phenolic resin are tabulated below.

Reaction i	ρ_{o_i} (lbm/ft³)	ρ_{r_i} (lbm/ft³)	B_i (sec⁻¹)	ψ_i	E_{a_i}/R (°R)	Γ
1	1.8965	0	0.77715	0.91273	5522.17	
2	79.6735	67.4994	7.791	0.96349	13005.18	1.0
3	–	–	–	–	–	

b) The following equation is suggested for layup angles other than 0° and 90°

$$k_\theta = k_{0°}\left\{1 + \left(\frac{k_{90°}}{k_{0°}} - 1\right)\sin\theta\right\}$$

where θ is the layup angle referenced to a tangent to the surface.

c) The conductivity is given by

$$k = x\, k_p(T) + (1 - x)k_c(T)$$

where x is the virgin material mass fraction, and k_p and k_c are the virgin material and char conductivity, respectively.

TABLE 5-8. THERMAL AND PHYSICAL PROPERTIES OF HYBRID PITCH MAT/RAYON FABRIC PHENOLIC

Material	Nominal Density (lb/ft³)	Nominal Resin Mass Fraction	Heat of Formation (Btu/lbm)	Resin Elemental Formula (Phenolic)	Reinforcement Elemental Formula	Fail Temperature (°R)	Virgin Material					Char			
							Temperature (°R)	Specific Heat (Btu/lbm-°R)	Thermal Conductivity x10⁴ (Btu/ft-sec-°R) 0° layup	Thermal Conductivity x10⁴ (Btu/ft-sec-°R) 90° layup	Emissivity	Specific Heat (Btu/lbm-°R)	Thermal Conductivity x10⁴ (Btu/ft-sec-°R) 0° layup	Thermal Conductivity x10⁴ (Btu/ft-sec-°R) 90° layup	Emissivity
Hybrid Pitch Mat/Rayon Fabric Phenolic FM5790	93.510	0.192	-476.52	C_6H_6O	C	—	530	0.160	1.03	2.20	0.85	0.210	0.30	14.00	0.85
							800	0.360	1.23	2.62		—			
							1000	0.420	1.30	2.75		0.430			
							1200			2.77		—			
							1600					0.470			
							2000					0.484			
							3000					0.493			
							4000					0.498	0.40	13.75	
							5000					0.500	0.70	11.60	

a) The decomposition kinetic constants for phenolic resin are tabulated below.

Reaction i	ρ_{oi} (lbm/ft³)	ρ_{ri} (lbm/ft³)	B_i (sec⁻¹)	ψ_i	E_{ai}/R (°R)	Γ
1	2.375	0	4.8	0.358	7787.6	
2	91.135	75.560	3.5712×10^6	2.259	27825.0	1.0
3	—	—	—	—	—	

b) The following equation is suggested for layup angles other than 0° and 90°

$$k_\theta = k_{0°}\left\{1 + \left(\frac{k_{90°}}{k_{0°}} - 1\right)\sin\theta\right\}$$

where θ is the layup angle referenced to a tangent to the surface.

c) The conductivity is given by

$$k = x\, k_p(T) + (1 - x)k_c(T)$$

where x is the virgin material mass fraction, and k_p and k_c are the virgin material and char conductivity, respectively.

TABLE 5-9. THERMAL AND PHYSICAL PROPERTIES OF PITCH MAT MOLDING COMPOUND

Material	Nominal Density (lb/ft³)	Nominal Resin Mass Fraction	Heat of Formation (Btu/lbm)	Resin Elemental Formula (Phenolic)	Reinforcement Elemental Formula	Fail Temperature (°R)	Virgin Material					Char			
							Temperature (°R)	Specific Heat (Btu/lbm-°R)	Thermal Conductivity x10⁴ (Btu/ft-sec-°R) 0° layup	Thermal Conductivity x10⁴ (Btu/ft-sec-°R) 90° layup	Emissivity	Specific Heat (Btu/lbm-°R)	Thermal Conductivity x10⁴ (Btu/ft-sec-°R) 0° layup	Thermal Conductivity x10⁴ (Btu/ft-sec-°R) 90° layup	Emissivity
Pitch Mat Molding Compound MXC313P	88.417	0.190	-433.20	C_6H_6O	C	–	530	0.160	1.30	2.10	0.85	0.210	3.65	11.25	0.85
							800	0.360	1.50	2.60		–			
							1000	0.420	1.50	2.72		0.430			
							1200					–			
							1400					0.470			
							2000					0.484			
							3000					0.493	4.00	12.00	
							4000					0.498	5.00	13.90	
							5000					0.500	6.70	16.75	

a) The decomposition kinetic constants for phenolic resin are tabulated below.

Reaction i	ρo_i (lbm/ft³)	ρr_i (lbm/ft³)	B_i (sec⁻¹)	ψ_i	E_{ai}/R (°R)	Γ
1	2.4756	0	164.464	2.5591	8302.88	
2	8.5764	0	4.884×10^9	1.2265	35541.80	0.5
3	165.7818	143.2356	1.70007×10^{22}	6.9232	64876.00	

b) The following equation is suggested for layup angles other than 0° and 90°

$$k_\theta = k_{0°}\left\{1 + \left(\frac{k_{90°}}{k_{0°}} - 1\right)\sin\theta\right\}$$

where θ is the layup angle referenced to a tangent to the surface.

c) The conductivity is given by

$$k = x\,k_p(T) + (1 - x)k_c(T)$$

where x is the virgin material mass fraction, and k_p and k_c are the virgin material and char conductivity, respectively.

TABLE 5-10. THERMAL AND PHYSICAL PROPERTIES OF PITCH FABRIC PHENOLIC

Material	Nominal Density (lb/ft³)	Nominal Resin Mass Fraction	Heat of Formation (Btu/lbm)	Resin Elemental Formula (Phenolic)	Rein-forcement Elemental Formula	Fail Temperature (°R)	Virgin Material					Char			
							Temperature (°R)	Specific Heat (Btu/lbm-°R)	Thermal Conductivity x10⁴ (Btu/ft-sec-°R) 0° layup	Thermal Conductivity x10⁴ (Btu/ft-sec-°R) 90° layup	Emissivity	Specific Heat (Btu/lbm-°R)	Thermal Conductivity x10⁴ (Btu/ft-sec-°R) 0° layup	Thermal Conductivity x10⁴ (Btu/ft-sec-°R) 90° layup	Emissivity
Pitch Fabric Phenolic MXG1033F	102.260	0.119	-379.05	C_6H_6O	C	—	530	0.120	1.30	2.90	0.85	0.210	1.60	18.75	0.85
							800	0.320	1.45	2.94		—			
							1000	0.380	1.50	3.24		0.430			
							1200	0.430	1.50	3.43		—			
							1400	0.440		3.45		0.470			
							2000					0.484			
							3000					0.493		17.25	
							4000					0.498		12.30	
							5000					0.500	1.20	7.20	

a) The decomposition kinetic constants for phenolic resin are tabulated below.

Reaction i	ρ_{o_i} (lbm/ft³)	ρ_{r_i} (lbm/ft³)	B_i (sec^{-1})	ψ_i	E_{a_i}/R (°R)	Γ
1	1.0226	0	6.4977×10^4	0.838	12095.0	
2	101.2374	90.3949	2.09904×10^6	2.667	23372.0	1.0
3	—	—	—	—	—	

b) The following equation is suggested for layup angles other than 0° and 90°

$$k_\theta = k_{0°}\left\{1 + \left(\frac{k_{90°}}{k_{0°}} - 1\right)\sin\theta\right\}$$

where θ is the layup angle referenced to a tangent to the surface.

c) The conductivity is given by

$$k = x\,k_p(T) + (1 - x)k_c(T)$$

where x is the virgin material mass fraction, and k_p and k_c are the virgin material and char conductivity, respectively.

TABLE 5-11. THERMAL AND PHYSICAL PROPERTIES OF CANVAS PHENOLIC

Material	Nominal Density (lb/ft³)	Nominal Resin Mass Fraction	Heat of Formation (Btu/lbm)	Resin Elemental Formula (Phenolic)	Reinforcement Elemental Formula	Fail Temperature (°R)	Virgin Material					Char			
							Temperature (°R)	Specific Heat (Btu/lbm-°R)	Thermal Conductivity x10⁴ (Btu/ft-sec-°R) 0° layup	Thermal Conductivity x10⁴ (Btu/ft-sec-°R) 90° layup	Emissivity	Specific Heat (Btu/lbm-°R)	Thermal Conductivity x10⁴ (Btu/ft-sec-°R) 0° layup	Thermal Conductivity x10⁴ (Btu/ft-sec-°R) 90° layup	Emissivity
Canvas Phenolic 4K9502	88.288	0.710	-1944.88	C_6H_6O	$C_6H_{10}O_5$	—	530	0.360	0.86	1.17	0.85	0.210	2.50	2.50	0.85
							800	0.440	0.90			—			
							1000	0.500	0.92			0.430			
							1200	0.540	0.93			—			
							1400					0.470			
							2000					0.484	5.00	5.00	
							3000					0.493	12.50	12.50	
							4000					0.498	19.75	19.75	
							5000					0.500	28.50	28.50	

a) The decomposition kinetic constants for phenolic resin are tabulated below.

Reaction i	ρ_{o_i} (lbm/ft³)	ρ_{r_i} (lbm/ft³)	B_i (sec⁻¹)	ψ_i	E_{a_i}/R (°R)	Γ
1	6.622	0	5.9285×10^2	1.091	10096.0	
2	88.906	0	2.39295×10^{11}	1.317	35602.0	0.5
3	81.048	51.206	2.37558×10^7	3.101	28225.0	

b) The following equation is suggested for layup angles other than 0° and 90°

$$k_\theta = k_{0°}\left\{1 + \left(\frac{k_{90°}}{k_{0°}} - 1\right)\sin\theta\right\}$$

where θ is the layup angle referenced to a tangent to the surface.

c) The conductivity is given by

$$k = x\, k_p(T) + (1 - x)k_c(T)$$

where x is the virgin material mass fraction, and k_p and k_c are the virgin material and char conductivity, respectively.

SECTION 6

CONCLUSIONS

In summary, the following conclusions can be extracted from this study:

- With the exception of molding compounds and Kureha fabric, all carbon phenolics perform equal to or better than MX4926 in the APG.
- With the exception of hybrid materials the performance of a particular generic class was not especially dependent upon the material supplier.
- Higher mass losses in the 90° orientation are due to thicker char formations (higher conductivities).
- Kynol materials had satisfactory thermal performances in the APG, but they are not really low cost materials. However, these materials may be considered as good alternate materials.
- Pitch carbon mat materials have a combination of good performance and low cost.
- There was a large variance in residual volatile measurements but no obvious correlation between this and ablation performance was found. However, post-cured materials generally performed better than as received materials.
- Data required for thermal performance predictions were determined for thermal conductivity (both 0° and 90° orientations), specific heat, density, pyrolysis kinetics, heat of formation, and pyrolysis gas elemental composition. These data will subsequently be used as inputs to the Aerotherm computer codes (ACE and CMA).

REFERENCES

1. Moyer, C. B. and Rindal, R. A.: "An Analyses of the Coupled Chemically Reacting Boundary Layer and Charring Ablator, Part II Finite Difference Solution for the In-Depth Response of Charring Materials Considering Surface Chemical and Energy Balances," NASA CR-1061 (Aerotherm Final Report 66-7, Part II), June 1968.

2. Schaefer, J. W. and Dahm, T. J.: "Studies of Nozzle Ablative Material Performance for Large Solid Boosters," NASA CR-72080 (Aerotherm Report No. 66-2), December 15, 1966.

3. Baker, D. L., Wool, M. R., and Schaefer, J. W.: "A Dynamic Technique for Determining the Thermal Conductivity of Charring Materials," Paper presented at the Eighth Conference on Thermal Conductivity, October 7-11, 1968, Thermophysical Properties Research Center, West Lafayette, Indiana.

4. McCuen, P. A., Schaefer, J. W., Lundberg, R. E., and Kendall, R. M.: "A Study of Solid-Propellant Rocket Motor Exposed Materials Behavior," Report No. AFRPL-TR-65-33 (Vidya Report No. 149), February 26, 1965.

5. Schaefer, J. W., et al.: "Studies of Ablative Material Performance for Solid Rocket Nozzle Application," NASA CR-72429 (Aerotherm Report No. 68-30), March 1, 1968.

APPENDIX A

RESIDUAL VOLATILE MEASUREMENTS

Coded samples of each screening test material were sent to Hexcel Corporation for a determination of the residual volatile concentrations. These tests were performed in an attempt to resolve the anomalous arc plasma jet performance of MX4926 in the Series I tests. In these screening tests, MX4926 exhibited severe delamination when convectively heated with the fabric plys parallel to the flow direction. This delamination was of special concern since all other materials exhibited little or no delamination problems. The residual measurement was one of two steps being taken to determine the reasons for this delamination.

The residual tests were conducted by crushing appropriate size samples which were then desiccated for 48 hours and weighed. These dried samples were heated at 325°F for 4 hours, removed from the oven and desiccated for an additional 3 hours and weighed again. The percentage weight loss was defined as the percent residual volatiles content. In some cases, two measurements were made on the same material (but not necessarily the same physical block) to determine consistency. Since the cure size may influence the magnitude of the residuals the approximate dimensions of the as-received materials are shown along with the volatiles content in Table A-1. For cases where two samples were measured the block sizes of each sample, if different, are also shown.

From Table A-1 it can be seen that the measurement repeatability was very good when samples were taken from the same size blocks. However, there is some dependence on block size as seen in sample numbers 2, 5, 12, and 14. The Fiberite materials showed consistently higher volatile contents for 2" diameter samples than for flat blocks (e.g., 4 x 4 x 1-1/2). The reverse is true for the Hexcel material although only 1 material was tested redundantly.

The residuals content of the MX4926 was the lowest of all materials tested. This measured value of 0.56 percent may be compared with a value of 1.1 percent as measured by Fiberite. This difference is probably due to measurement techniques since there is no industry-wide accepted standard for residual volatiles measured techniques. The significance of the reported measurements is that all materials were measured under identical conditions and can therefore be ranked in a relative

TABLE A-1. SCREENING MATERIAL RESIDUAL VOLATILE MEASUREMENTS

Number	Material	Supplier	Designation	As Received Dimensions*	% Residual Volatiles
1	Pitch Mat/Phenolic	USP	FM5782BG	5-1/2 x 5-1/2 x 3/8	2.05
2	Pitch Mat/Phenolic	Fiberite	MX4929	4 x 4 x 1-1/2	1.15/1.40
3	Pitch Mat/Phenolic	Ferro	ACX-C86PM	2-1/2 x 2-11/16 x 1-7/8	1.38/1.39
4	Hybrid	Hexcel	4CSP08/4C1008	2-1/8 x 1-3/16 x 1-5/16	1.49/1.45
5	Hybrid	Fiberite	MX4928	2D x 1-3/4	1.97/1.44
6	Hybrid	USP	FM5790	6 x 6 x 1-1/4	2.81
7	Kynol/Phenolic	Ferro	ACX-CPH	~4 x 4 x 3	1.45/1.47
8	Kynol/Phenolic	USP	XFM5795	6 x 6 x 1-1/4	5.41
9	Kureha/Phenolic	Ferro	ACXCB6K	2-1/2 x 2-11/16 x 1-7/16	4.08/4.00
10	Molding Compound	USP	FM5782MC	2D x 1-3/4	1.76
11	Molding Compound	Fiberite	MXC313P	2D x 1-3/4	1.08
12	Molding Compound	Hexcel	4CSP08MC	3D x 1-1/2 2-3/8 x 1-3/8 x 1-3/8	1.44/1.69
13	Molding Compound	Ferro	ACX-CB6PMC	4 x 4 x 2	2.33
14	Silica/Phenolic	Fiberite	MX-260D	2D x 1-7/8 4 x 4 x 1-1/2	4.19/1.23
15	Silica/Phenolic	Ferro	CA/2221/96	1-9/16 x 2-3/8 x 1-3/4	2.22
16	Silica/Phenolic	Fiberite	MXSE-55	4 x 4 x 1-1/4	1.83
17	Canvas/Phenolic	Hexcel	4K9502	4 x 4 x 1	4.26
18	Canvas/Phenolic	Fiberite	MXKF-418	4 x 4 x 1-1/4	4.12
19	Canvas/Phenolic	Fiberite	MX4926	2D x 1-3/4	0.56

*First 2 dimensions define plane of fabric or mat layup. Cylindrical samples have layup perpendicular to axis.

sense. Since the residual's content of MX4926 was lower than the other materials, the delamination problem cannot be attributed to a high volatile content. Since there is no rationale for relating delaminations to low volatiles content, it is concluded that volatiles evolution during APG testing did not cause the observed delaminations.